

High-resolution imaging of ultracold atoms

Tom Matty Bo Asmussen
toasm15@student.sdu.dk

BSc Student

SDU Engineering

Physics and Technology

Supervisors:

René L. Eriksen

Sebastian Hofferberth

1st June 2018

Abstract

This research looks at a new imaging system created for the Rydberg quantum optics experiment at SDU. The system is a long working distance high-resolution imaging objective used for the characterization of an atomic sample. This thesis is concerned with the characterization of this objective after it is implemented into a previously designed mount. The characterization is performed by calculating the contrast of an image for small resolution patterns. Several results display contrasts which exceeds the theory. The investigations indicate that these deviations stem from options in the camera and the camera's response function. The best resolvable resolution obtained in this project through the objective is $3.91\mu\text{m}$, which does agree with Abbes diffraction limit on the system.

Contents

1	Introduction	4
2	Construction of the Imaging system	5
2.1	Design	5
2.1.1	Objective	5
2.1.2	Components	6
2.2	First Set-up	6
3	Optical theory and pre analysis	9
3.1	Optical software for layout and optimization (OSLO)	9
3.2	Focal point and magnification	9
3.3	Reviewing OSLO's simulation through cardinal points	10
3.3.1	Ray-transfer Matrices	10
3.3.2	Cardinal Points	11
3.3.3	The comparison	12
3.4	Optical resolution	12
3.5	Component characteristics and Sensitivity	14
3.6	Modulation-Transfer-Function	18
4	Imaging setup in new mount	21
4.1	New Set-up	21
4.2	Raspberry Pi-Camera	22
4.2.1	Location significance	22
4.2.2	Focus shift	23
4.3	Image analysis	24
4.4	Absorptive Neutral Density Filters	26
4.5	Gamma correction	28
4.6	Diffuser	29
5	Discussion	32
5.1	Adding of an extra lens	32
5.2	Optimized distance between the objective and 750mm lens	32
5.3	Camera response function	32
5.4	Diffuser	32
6	Conclusion	33
7	Acknowledgment	34
A	1951 USAF resolution test chart look up table	36
B	Table of ray-transfer matrices	36
C	Significance of vanishing ray-transfer matrix elements	37
D	Cardinal points table	37
E	Image of resolution chart obtained by F. Christaller	38
F	Acronyms	39
G	List of symbols	40

1 Introduction

The research group, under which supervision this project was undertaken, work with the research of the Rydberg atom where manipulation of light in ultracold gases happens at a single-photon level. Because of specific requirements, a custom imaging system had to be constructed, which then is used for the imaging of the atomic samples, which then can be characterized for their number of atoms, temperature, and shape. It should be able to detect a small atom cloud inside a vacuum chamber, while itself being on the outside. To have the objective inside the chamber would restrain the lowest obtainable pressure inside the cell and once inside, the adjustment of the optical system under vacuum would not be possible. A compound of lenses which included the vacuum cell as an element was firstly designed by W. Alt[Alt02] for an efficient detection of single atoms. This was further developed by Pritchard, Isaacs, and Saffman [PIS⁺17], which can be adapted to a wide range of wavelengths. This system of lenses is designed to be diffraction limited with a long working distance. The high-resolution imaging for the experiment was optimized further by F. Christaller [Chr17] for a vertical axis imaging for the Rydberg experiment on SDU, which was done with the ray tracing program OSLO. In this thesis there will be assembled the from F. Christaller created objective lens system inside a mount, go through some theory behind obtaining resolution and characterizing sensibility, and afterwards characterizing the images from a resolution test target made with the new objective. In this particular experiment, the imaging of the Rubidium cloud is performed on the 780nm transition.

2 Construction of the Imaging system

In this section a brief introduction to the different optical components and first set-up used to characterize the objective before setting into its pre designed mount.

2.1 Design

Figure 1 shows the main part of the set-up, which was simulated with OSLO. It shows the different components and the rays propagation through them. In the real experiment the goal is to image an atom cloud. This will be represented as a resolution test chart target. The ultracold atom cloud is trapped inside a vacuum chamber. As mentioned before, it would be troublesome to have the objective inside the vacuum, so the rays travel through a glass-cell and continue towards a waveplate and polarizing beamsplitter. The reason behind the distance between the waveplate and glass-cell is that there will be a magneto-optical trap right after the glass-cell. After the beamsplitter we will have a tube containing the 4 lenses used to form the objective. All the distances have been optimized by the use of OSLO. The next chapter will go through some of the different components here mentioned and the ones not seen on figure 1.

2.1.1 Objective

The objective is a compound of 4 lenses mounted inside a *Thorlabs* tube. The lenses used are:

1. **Thorlabs LE1202-B** | Positive Meniscus Lens, $f = 200$ mm
2. **Thorlabs LA1708-B** | Plano-Convex Lens, $f = 200.0$ mm
3. **Thorlabs LB1294-B** | Bi-Convex Lens, $f = 175.0$ mm
4. **Newport KPC028AR.16** | Plano-Concave Lens, $f = -200$ mm

The lenses are all of the size of 1 inch and are standard lenses from the commercial catalogue from *Thorlabs* and *Newport*. The first 3 lenses are fixed in place by distance rings between them, while the fourth lens is mounted separately, so it could be adjusted until the image firstly was set in focus and since then likely not been changed. The lenses had already been assembled by F. Christaller.

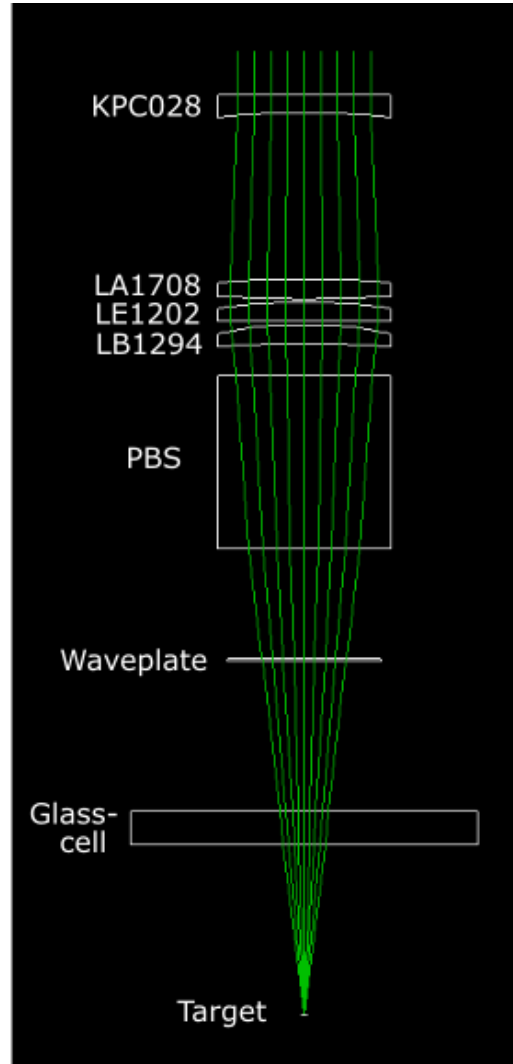


Figure 1: Illustration of the light-rays migration from the target to and through the objective together with the different optical objects it moves through. Image taken with the OSLO

2.1.2 Components

Test Target: In the test set-up, a 1951 USAF resolution chart is used to represent the atom cloud. This is a resolution test chart with several 3 stripe patterns in both the vertical and horizontal axes, arranged in groups consisting of 6 elements. With a given element inside a group, the resolution can be found by

$$\text{Resolution}(lp/mm) = 2^{\text{group} + \frac{\text{element} - 1}{6}} \quad (1)$$

The higher the group number, the smaller is the size of a single line. In Appendix A a lookup table can be found for numbers of line pairs per mm for a given element in a group.

The resolution chart was mounted on a 3D translation stage to find the focus and the pattern on the chart more easily.

Glassplate: Representation of the surface of the vacuum chamber as it is in the Rydberg experiment set-up

Beam splitter: Just before the objective, there is placed a polarizing beamsplitter (PBS), which splits the laser into two directions, depending on the incoming polarization.

Waveplate: To adjust the laser's incoming polarization, a $\lambda/2$ waveplate is placed with a short gap in front of the PBS. While working with the objective in this project, the waveplate is adjusted so that all the light from the laser will go through the PBS into the objective.

Diffuser: Used to scatter light and reduce the spatial coherence of the laser light. Normally coherent light is desirable, but in this experiment we are not interested in the light itself, but in the shadow that's being cast, which is imaged best without coherent light. It is because the Huygen wave-fronts interfere with themselves after going through slits creating interference patterns and the resolution chart is basically full of slits. The coherence itself can be reduced by making the laser go through an uneven surface. It can reduce the interference effect even more by having the surface rotate and thereby making the light more random in a way. [SZD+17]

Laser: A Laser with a wavelength of 780nm, which intensity is adjustable.

Additional lens: there is a 750mm plano-convex lens mounted after the objective, to refocus the image towards the camera. Often referred to the focussing lens in this thesis.

Camera: The camera is a Raspberry Pi Camera Module v2 with a 3280×2464 px chip and a pixel size of $1.12 \times 1.12 \mu\text{m}^2$. The initial settings of the camera were in automatic. A table with the optimized distances between the components by the simulation software can be seen on the next page on table 1.

2.2 First Set-up

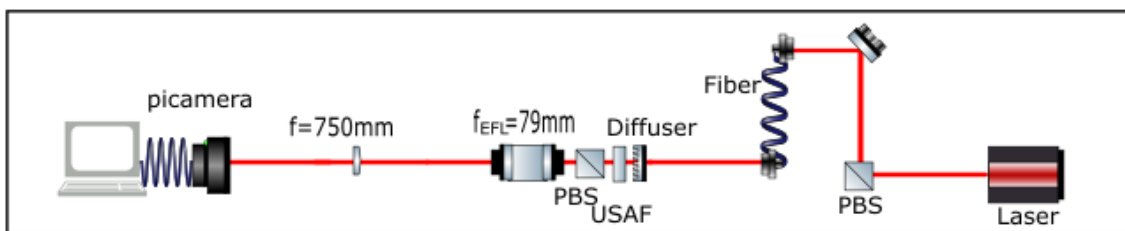


Figure 2: A drawing of the set-up with the different components used in the recreation of the set-up.

The first set-up where the initial objective tube with the lenses was tested can be seen on figure 2. This system has been constructed beginning with the laser. The first thing one should pay attention to when working with optical systems, is to be thoroughly with the alignment of the laser beam. The set-up is placed on a breadboard, where the components can be mounted on. Since the output laser from a couple of the components can be adjusted in more than one dimension, one would then align the laser in a way that the height of it in respect to the surface of the board would stay the same. The outgoing beam from the laser is measured to have a height of 100mm, which then should be maintained throughout the whole set-up. To align the light from the laser, one would try to align the laser above the holes. Every time another object is being added, it should be aligned, so that it follows the path of holes for as far as possible and at the same time keeps the height, before the next one is being added.

Table 1: Surface data from the different elements of the system from the target to the objective as designed by F. Christaller and optimized through OSLO. Every surface is given a number with a thickness and aperture radius. Surface 2 and 8 are the optimized distances. Adopted from [Chr17]

Surface	Element	Thickness [mm]	Aperture radius [mm]	Glass
Object	–	1.0000e+20	8.7269e+17	Air
1	NKPC028	2.500000	12.700000	N-BK7
2		24.381423	12.700000	Air
3	TLVISLB1294	2.900000	12.700000	N-BK7
Aperture stop		0.500000	10.950000	Air
5	TLVISLA1708	2.780000	12.700000	N-BK7
6		0.500000	12.700000	Air
7	TLVISLE1202	2.790000	12.700000	N-BK7
8		4.569877	12.700000	Air
9	PBS cube	25.400000	12.700000	N-SF1
10		16.000000	12.700000	Air
11	$\lambda/4$ waveplate	0.500000	11.300000	Quartz
12		5.600000	11.300000	Air
13	aperture of MOT-coils	16.100000	14.500000	Air
14	glass cell	5.000000	25.400000	Quartz
15		0.000000	25.400000	Air
Image	–	25.000000	0.696625	

The picture taken with the Pi camera from the target is seen on figure 3. In the image is a lot of interference, as seen as the black circular rings all over the picture, which ideally should be perfectly white.

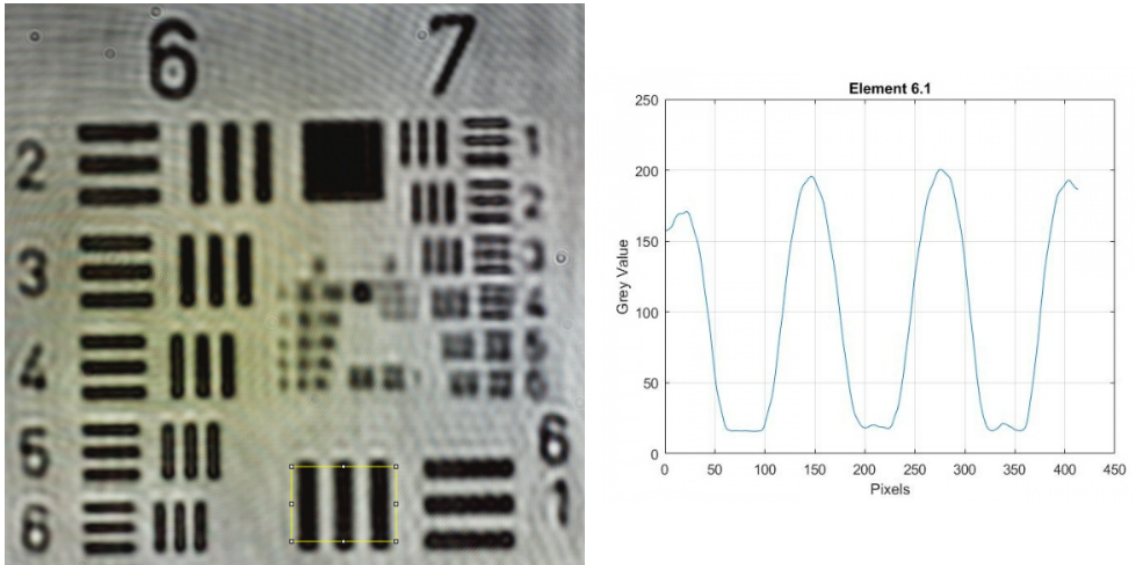


Figure 3: Here seen is an image of the resolution chart (left) together with a profile plot of one of the stripe patterns (right). On the resolution chart is the area of the vertical lines in element 6.1 marked for being analysed. The plot profile shows the gray value in respect to the position displayed as pixels.

To the Left is the resolution chart imaged by the camera and to the right is a plot diagram relating to the grey-scale of the line pattern going from left to right in Element 6.1. The program used to produce the plot profile is ImageJ, which uses the average of all horizontal lines in the targeted area. That picture can then be used to describe the possible achievable resolution. The methods used to do so will be described in the next chapter.

3 Optical theory and pre analysis

This chapter will start with theoretical background on optical imaging and will cover areas like component sensibility, measurement of resolution, and the simulation software OSLO. Some of the specific things that will be investigated is the importance of the placement of the fourth lens in respect to the third (Surface 2 in table 1). If it's placement is critical for the performance of the objective, it might be taken into account to change the location to achieve a better resolution of the image. Furthermore methods of defining the resolution of an optical system will be undertaken.

3.1 Optical software for layout and optimization (OSLO)

To ensure the right distances with the best resolution and least amount of aberrations, a ray tracing software called OSLO (Optical software for layout and optimization [Lam12]) was used by F. Christaller to optimize the objective for the criteria on high-resolution imaging for the vertical axis for the experiment of Rydberg atoms. OSLO is a lens design software used for several simulations and analysis of performances of optical systems. OSLO has a spreadsheet in which the desired lenses can be added to with the data for thickness and aperture radius and material as seen in table 1. The most commercial available lenses for example Thorlabs and Newport are accessible through OSLO's catalogue, so the data for the lenses don't have to be added manually. Afterwards one would enter the given distances between the lenses and defining variables the software should use for the optimization. In the executed simulation two distances were established as variable, which the program would optimize, until the best resolution with the least amount of aberrations was found. The only two variables in the optimization were the distance between the last and second to last lens and the distance between the whole objective in respect to the beamsplitter. In respect to table 1 these were surface 2 and 8. Furthermore than the distances, one can access several analyses, like the cardinal points of the system, spot diagrams, and a modulation transfer function which are described and used later in this chapter.

3.2 Focal point and magnification

When faced with a problem, a good idea would be to start with the easiest and cheapest solution and see if it satisfies the criteria of task. In the case of a magnification, the simplest solution would be a single lens. When faced with the goal to get a given magnification one would then use the following equation taken from chapter 2 in introduction to optics [PPP]

$$M = -\frac{s'}{s} \quad (2)$$

where m is the magnification, s is the distance from the objective to the lens, and s' is the distance from the lens to the image, as seen on figure 4. The minus tell us, that the image is flipped compared to the object.

To find the focal length, F , one would use the thin lens equation, which states the relationship between the two distances s and s' in respect to the focal length.

$$\frac{1}{s} + \frac{1}{s'} = \frac{1}{F} \quad (3)$$

To get an even better estimate of the focal length, one could use the lensmaker's equation, where you include the refractive indexes of the medias the ray travels through and the curvature of the lenses surfaces.

An optical system of 2 lenses is seen as an optical telescope. A telescopes angular magnification is given by:

$$M = \frac{f_0}{f_e} \quad (4)$$

where f_0 is the focal length of the objective lens and f_e the focal length of the eyepiece, which can be seen as the focal length of lens 1 and 2 in a two lens system. For high resolution imaging and confined space, a two lens system is often not viable, which is why the objective in this setup

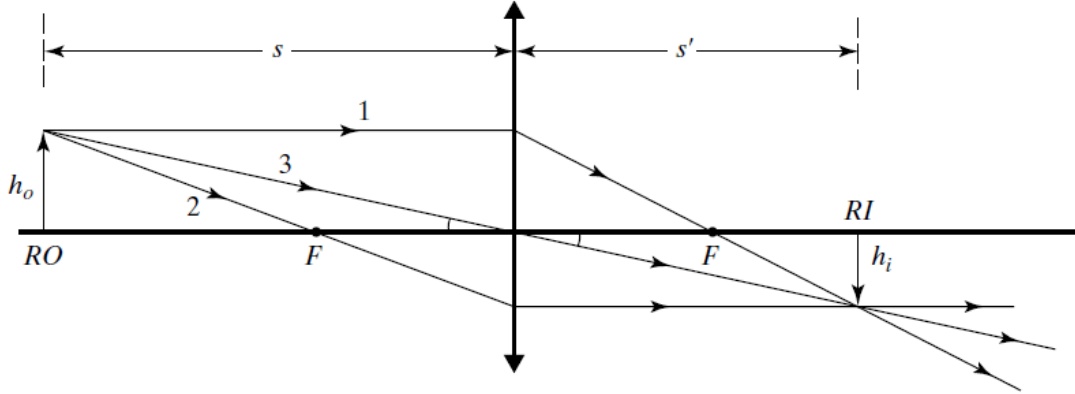


Figure 4: Ray diagram by a convex lens. RO is the real object with a height of h_o and RI is the real image with a height of h_i in respect to the axis. F is the focal length of the lens and s and s' are the distances between the lens and respectively RO and RI. Image adopted from chapter 2 of [PPP]

is consisting of 4 lenses optimized to small value of the limit of diffraction and aberrations. The magnification of the setup is:

$$M = \frac{f_{Fcs}}{f_{EFL}} \quad (5)$$

$$= \frac{750mm}{79.75mm} = 9.4 \quad (6)$$

Where f_{Fcs} is the lens used for focusing the image to the camera and f_{EFL} is the effective focal length of the objective. The effective focal length of several lenses combined can be found by the use of a ray-transfer matrix, which will be discussed in the next section.

3.3 Reviewing OSLO's simulation through cardinal points

For dealing with optical systems of containing several different surfaces and refractive indexes, the matrix method is used to represent the whole system a single thick lens with a 2x2 matrix, which elements can be used to find the cardinal point of the represented lens. This subsection will go through the process of finding the cardinal points of the used optical system in this project by all the used components and compare the result with the OSLO software.

3.3.1 Ray-transfer Matrices

The matrix which characterizes the optical system is used to describe what happens to a single ray of an 1x2 vector, with the input values of its height and angle in respect to the optical axes. This vector multiplied with the matrix will result in a new vector, which belongs to the outgoing ray, after having traveled through the system, which is written as:

$$\begin{bmatrix} y_f \\ \alpha_f \end{bmatrix} = \mathbf{M} \begin{bmatrix} y_0 \\ \alpha_0 \end{bmatrix} \quad (7)$$

where y are the heights and α are the angles, where the left side is the outgoing ray and the right is the ingoing ray, where \mathbf{M} is the transfer matrix. The transfer matrix \mathbf{M} , that is used to describe the objective consisting of 4 lenses, is created by several matrices of the same dimension, which come from everything the ray passes through. A matrix is used every time the laser ray propagates through a medium like glass or air in a so-called translation matrix. Every time it is refracted on a surface a refraction matrix is used. A table of some of the simple ray-transfer matrices, like the ones just named can be found in Appendix B and are used to calculate the transfer matrix of the objective, by multiplying the matrices together, like the following:

$$\mathbf{M} = \mathbf{M}_N \mathbf{M}_{N-1} \cdots \mathbf{M}_2 \mathbf{M}_1 \quad (8)$$

where you multiply them one after another as they appear in the system backwards, with the last element first and the first element last. The resulting matrix will then look like the following:

$$\mathbf{M} = \begin{bmatrix} A & B \\ C & D \end{bmatrix} \quad (9)$$

with A to D as the matrix elements. The resulting matrix elements can then be used to find the cardinal points of the imaginary lens that represents the optical system, which is described further in the following section. Taking equation 7 and 9 we get following relations:

$$\begin{aligned} y_f &= Ay_0 + B\alpha_0 \\ \alpha_f &= Cy_0 + D\alpha_0 \end{aligned} \quad (10)$$

In Appendix C figure 38 it is shown how rays move through an optical system when specific element in the transfer matrix is 0. It would be good to end up with a matrix where the D value is close to zero, that would make sure that rays coming from the spot which we want to image to be collimated after the objective.

3.3.2 Cardinal Points

There are three types of cardinal points. These are focal points, principal points, and nodal points. The focal points and either the principal or nodal points of a lens can be used to characterize the behaviourism of the lens. There are two of each of these points, one for each of the corresponding surfaces. The lens these point are based on is a thick lens, which distance between the surfaces, compared to a thin lens, is not negligible. Where in a thin lens one would use the same focal length for each of its surfaces, the thick lens uses two different focal lengths, where one is the front focus (FF) and the other the back focus (BF), which are the two focal points. Seen on figure 5 is an image of a thick lens with the cardinal points and 3 different ray propagations. Its Nodal and principal plane is seen at the same location, because the principal plane depends on the difference between the refractive index before and after the lens. When its the same, as seen in the figure and as it is in this project, the two planes will be in the same position. The focal length, F , can be measured by subtracting the principal plane from the focal point. How the different cardinal points can be found through the matrix elements from the ray-transfer matrix and the relation between some of them can be seen in Appendix D on figure 39.

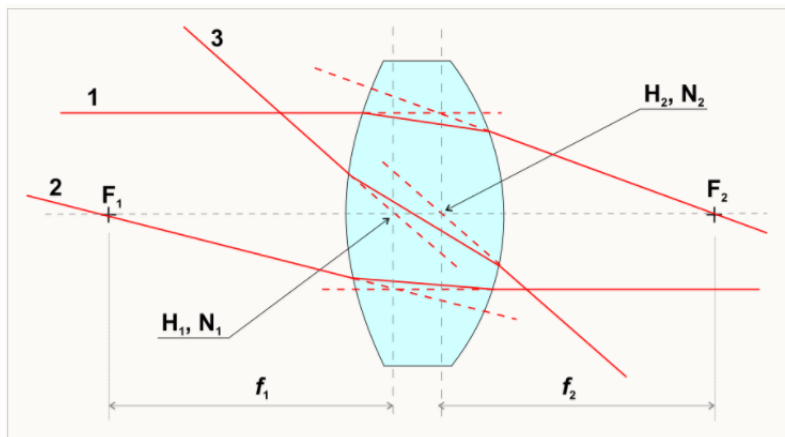


Figure 5: Here seen is the representation of a thick lens with F as the focal point for a given surface, H as the principal points, N as the nodal points, and f as the focal lengths. 3 rays' propagation through the lens is shown. The straight line is the actual way, while the dashed line is a presentation for, that one can approximate that the ray is only "broken" at the nodal/principal plane. Graphic taken from [Cos]

The same as for the thick lens seen in the above figure 5 applies to a system with several components. In comparison with the thin lens, the focal length in the thick lens or in a system with several components, the focal length of the system will be calculated from the principal planes instead of the surfaces. This gives the advantage when having an optical system of several surface,

that in confined space, the principal plane can be moved inside or out of the optical system, which is the case in this project.

3.3.3 The comparison

One would now be able to take the characteristics of the lenses and with them calculate the ray-transfer function. This is done by regarding all the lenses as thin lenses. With the data of the different focal length of the lenses and the distance between them, one can achieve the following ray transfer function by multiplying all the components' matrix as in eq 8:

$$\mathbf{M}_{objective} = \begin{bmatrix} 0.6107 & 78.946 \\ -0.0126 & 0.0080 \end{bmatrix} \quad (11)$$

To find the corresponding cardinal points to these matrix elements one can use the equations listed on figure 39 in Appendix C as mentioned before. To find the equivalent cardinal points from the OSLO simulation one can use the command (nodp) which prints the values of the cardinal points out for given surfaces, which in this case are the 4 lenses and their internal distances. On table 2 one can see the results of the thin lens matrix calculations and the results of OSLO's simulation.

Table 2: Cardinal points calculated through the matrix method compared to OSLO's values.

	EFL	N1	N2	FF	BF
Thin Lens Method:	79.332	30.881	9.3363	-48.451	88.668
Oslo:	79.7532	34.539	6.229	-45.215	85.982

One can see in the table that the different cardinal points and the effective focal length of the system is close to being the same. One could in theory improve the thin lens calculation by using thick lenses instead of thin lenses. That means for each thin lens matrix you would get a combination of 3 matrices; two refractive matrices and a translation matrix. This calculation was done, but from reasons unknown, a worse results for the cardinal points was achieved.

3.4 Optical resolution

To determine the resolution of an image, there are various ways it is defined. This section will discuss about what the best possible resolution for our system can be by going through the Rayleigh criterion, Abbes diffraction limit and numerical aperture. With the help of Rayleigh's criterion one can find out the limit of how close together two point sources can be to be *just* resolvable. To describe this, airy disc will be introduced. The use of a circular aperture in optics will yield a circular interference pattern in a ways that's called an airy pattern as seen on figure 6. the bright region in the middle is called the Airy Disc.

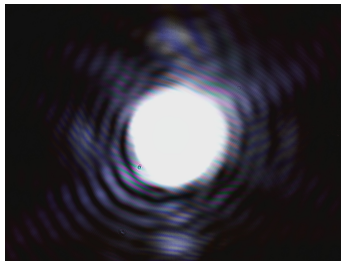


Figure 6: Here is an image of an airy disk with its circular pattern. Image taken with the experiments imaging setup with the use of an iris.

Rayleigh's criterion is defined that two point sources are regarded as just resolvable when the centre of the first airy disk overlaps with the first minimum of the interference of the second airy disk, as seen on figure 7. The centre of the airy disk is seen as the maximal intensity, which also counts for other diffractions than just the airy pattern. The first minimum of a circular diffraction pattern can be found by the following:

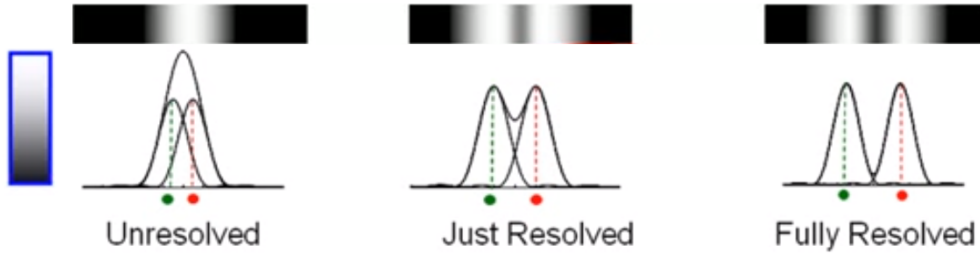


Figure 7: Here seen is a representation of Rayleigh's Criterion. With intensity graph from 2 different points in the bottom and the resulting image representation on top. The middle is Rayleigh's criterion, where the two different points are just resolvable. [Che]

$$\begin{aligned} \sin \theta_{\min} &= 1.22 \frac{\lambda}{D} \\ &\Downarrow \\ \theta_{\min} &\approx 1.22 \frac{\lambda}{D} \end{aligned} \quad (12)$$

Where θ is the angle from the incoming light, λ is the wavelength of the light, and D is the diameter of the lens' aperture. For small angles $\sin \theta$ is simplified to θ by small angle approximation. To translate the angle to the distance between the two objects, one would have to multiply angle with the distance from the lens to the object. By placing the object at the focal length of the objective we would obtain the following expression for the minimum distance between the objects:

$$x_{\min} = f \theta_{\min} = 1.22 \frac{f \lambda}{D} \quad (13)$$

where x_{\min} is the smallest observable distance between the two objects and f is the distance between the objects and the lens, which optimal would be the focal length, as illustrated in figure 8. Here one can see the the two object with the minimum distance between each other and the focal length distance to the lens. Furthermore to the right one can see the angle that corresponds to rayleigh's criterion, which is expressed by the intensity graph of the airy's.

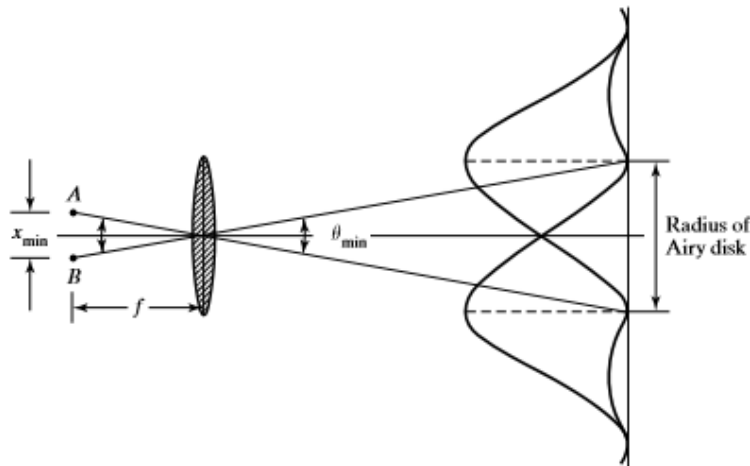


Figure 8: Here one can see two points, A & B, and the corresponding airy pattern as an intensity profile on the right. x_{\min} represents the minimal distance between the two points and θ_{\min} the minimal angle in respect to the rayleigh criteria. Image taken from chapter 11 of [PPP]

This can be further rewritten with the inclusion of the *numerical aperture* (NA). The numerical aperture is a dimensionless number, which describes the range of angles in which the objective can

collect and emit light. It is defined as:

$$\text{NA} = n \cdot \sin \theta = n \sin \left[\arctan \left(\frac{D}{2f} \right) \right] \approx n \cdot \frac{D}{2f} \quad (14)$$

where n is the refractive index of the medium in which the lens is located, in this case air ($n=1$) and θ is the angle between the optical axis and the last ray that still being collected by the objective.

The finest resolution able to be obtained, the Abbe diffraction limit, can be found by:

$$R = \frac{1.22\lambda}{2n \sin \theta} = \frac{1.22\lambda}{2\text{NA}} \quad (15)$$

Which shows that the numerical aperture should be as large as possible to increase the best possible resolution. This equation will be used later to define the best resolution obtainable by the objective system. The numerical aperture is found through the Oslo simulation to be 0.1216, which gives a diffraction limit of:

$$R = \frac{1.22\lambda}{2\text{NA}} = \frac{780\text{nm}}{2 \cdot 0.1216} = 3.91\mu\text{m} \quad (16)$$

3.5 Component characteristics and Sensitivity

This section will be about how big an impact it has when some components aren't in their optimal position and if it's negligible by moving other components to recover the best solution.

The way it is done in this project is to use OSLO's spot diagram. A spot diagram can be used to evaluate a lens quality in some form. It shows where how much rays from one point source spread out on the image. For the rays to form a good image, they have to end up close together. On figure 9 a spot diagram from OSLO's simulation on the optimized system is seen. The white circle is the airy disk. It is the best possible that could be achieved with a perfect lens and focus. Its size is defined by the diffraction limit, which was described earlier. To have the best possible image all rays must fall inside the circle.

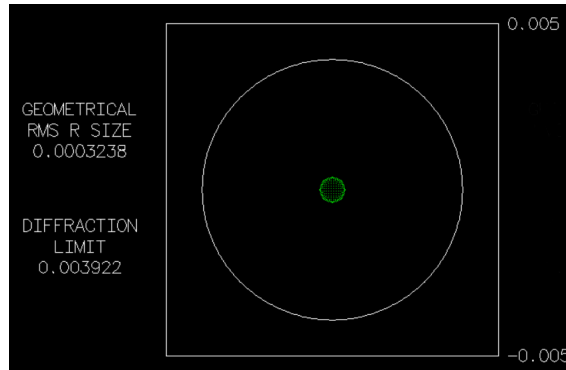


Figure 9: The spot diagram of OSLO's simulation of the optimized optical system. The green spots visualize the rays that end up as the image from the point source. The white circle represents the diffraction limit.

To use this as a sensitivity check, single parameters are changed and the change of the size of the ray bundle is noted. The first result of these is shown on figure 10, where the position between the last and second to last lens inside the four lens objective was changed. This has been done to find out how much influence the position of the last lens has, since once it's inside the objective tube and afterwards the mount, the lenses are no longer movable until it's disassembled from the mount. G_{rms} corresponds to the size of the ray bundle and D_{lim} is the diffraction limit, which only varies slightly in respect to the position change of the lens.

The graph results in a sensitivity of $13.8\mu\text{m}$ change of the radius of the ray bundle per mm change of the lens's location. The reason for the rays having a smaller radius with a minimal larger distance of the last lens is due to some aberrations. Another thing one can abstract from the graph is the interval in which the resolution is limited due to the diffraction limit. The interval

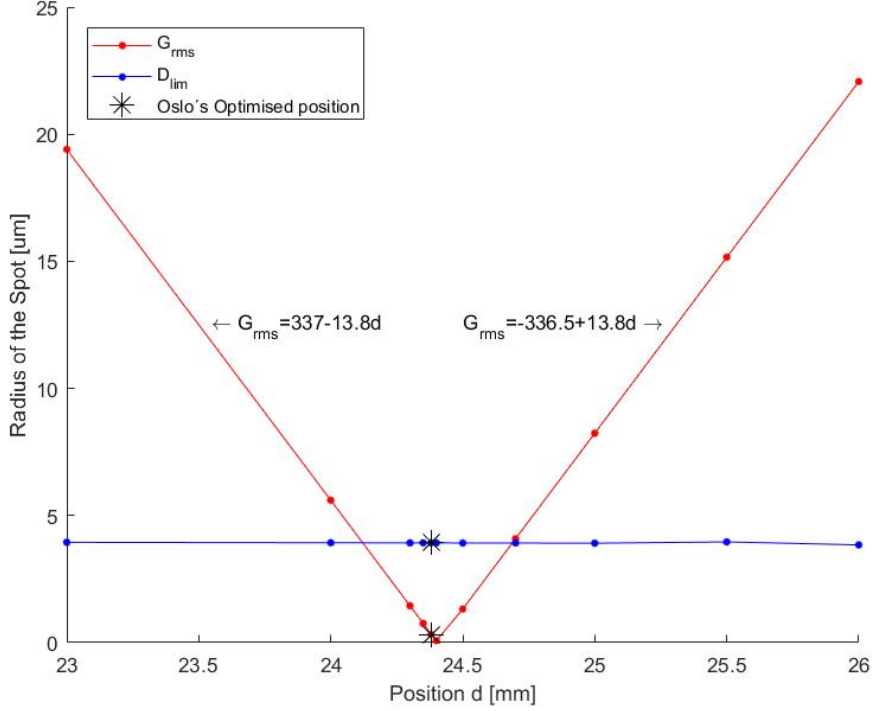


Figure 10: Distance change between Lens 3 and 4. Here seen are the values of G_{rms} and D_{lim} while the position between the second to last and last lens is varied. The black stars mark the area where Oslo optimized the best position to be.

corresponds to [24.1,24.7]. So this would conclude that the lens must have been placed within a 0.6mm interval. It would be interesting to check if the ray bundle could be maintained inside the diffraction limit by changing other parameters to compensate for the possible wrong distance between lens 3 and 4. The parameter which is used to check this is the distance between the objective and the PBS, which is also movable in the experiment compared to the lenses inside the objective, which aren't. This is seen on figure 11, where we have 4 different graph with their individual distance between Lens 3 and 4 with the variable change of the distance between the lens objective and PBS.

The red line in figure 11 is the optimized position between the lenses, with the starts indicating the associated optimized distance between the objective and PBS. The blue horizontal line represents the diffraction limit. The Graph shows that, regarding the spot diagram, the optimal resolution can still be obtained if lens 4 hasn't been placed perfectly in the objective by compensating it with the adjustment of the whole objective. The way it shows it is by having all of the other 3 graphs go below the diffraction limit at some position d.

The same has been done to see how big an impact it has if the glass-plate and PBS isn't sat in the predetermined position which is seen on figure 12 and 13. The results were similar to the previous gathered conclusion, that the consequence of an inaccurate location can be fixed by the adjustment of the objectives position in regard to the PBS and the other components to the left of the objective. Which is expected, as it is just a vertical surface that is being moved a bit to one side or the other. Its also seen in table 3 in Appendix ?? that for every mm the distance between the PBS and glass-plate gets changed, the same amount can be added/subtracted after the PBS to compensate for it.

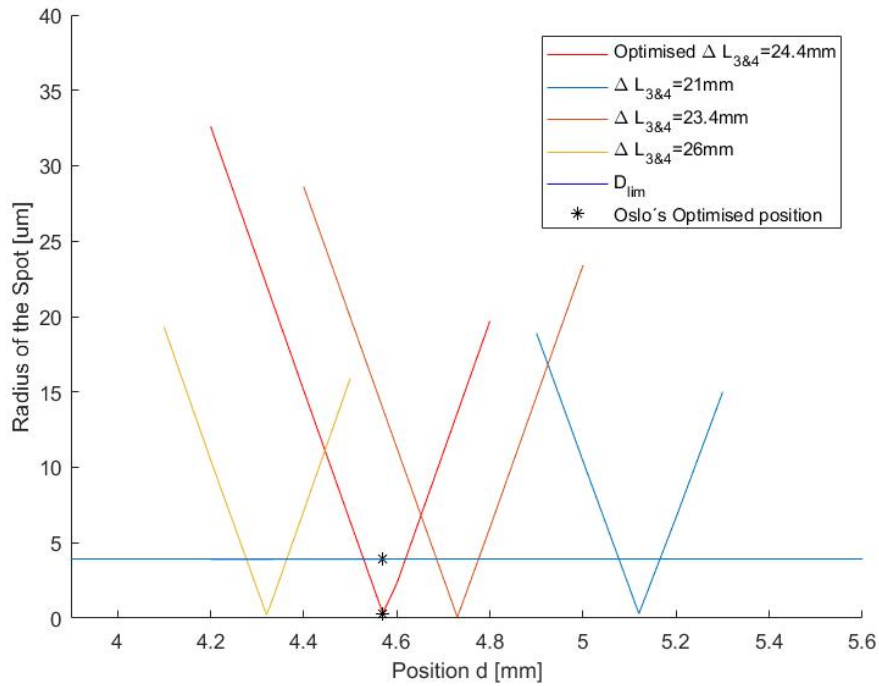


Figure 11: Graph of 4 different distances between Lens 3 and 4 and how the radius of the ray bundle changes in respect to change of distance between the combined 4 lens system and the PBS in each of the 4 graphs. The red one represents the optimized position between lens 3 and 4, with the black stars representing the optimal optimization.

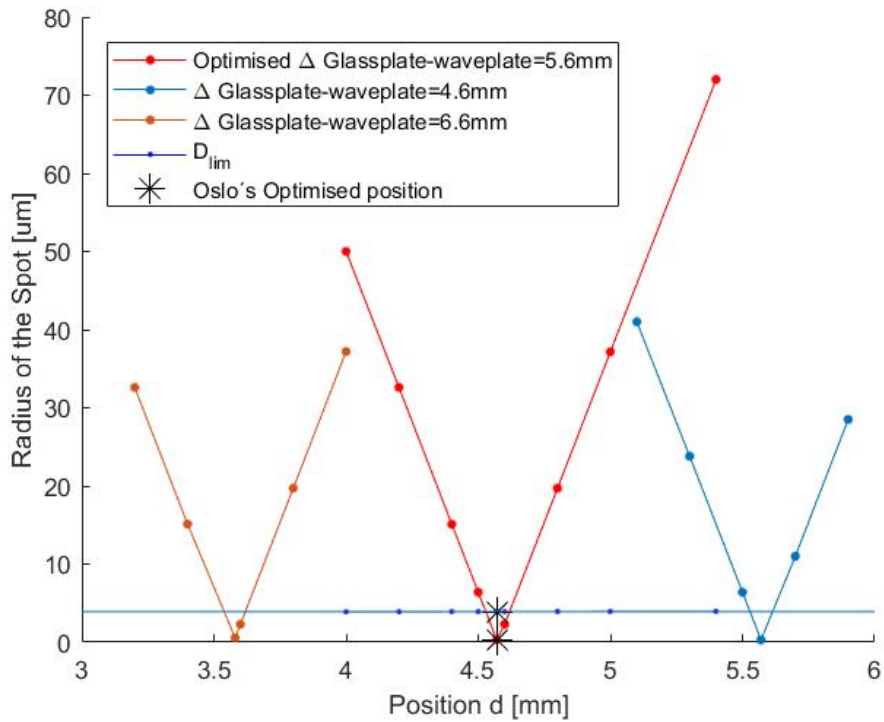


Figure 12: Radius of ray bundle in respect to a distance change between the PBS and objective. The 3 different data plots have different distances between the glass plate and the wave plate, which corresponds to surface 12 in 1. It is shown that the system can always be diffraction limited by adjusting the distance between the objective and PBS.

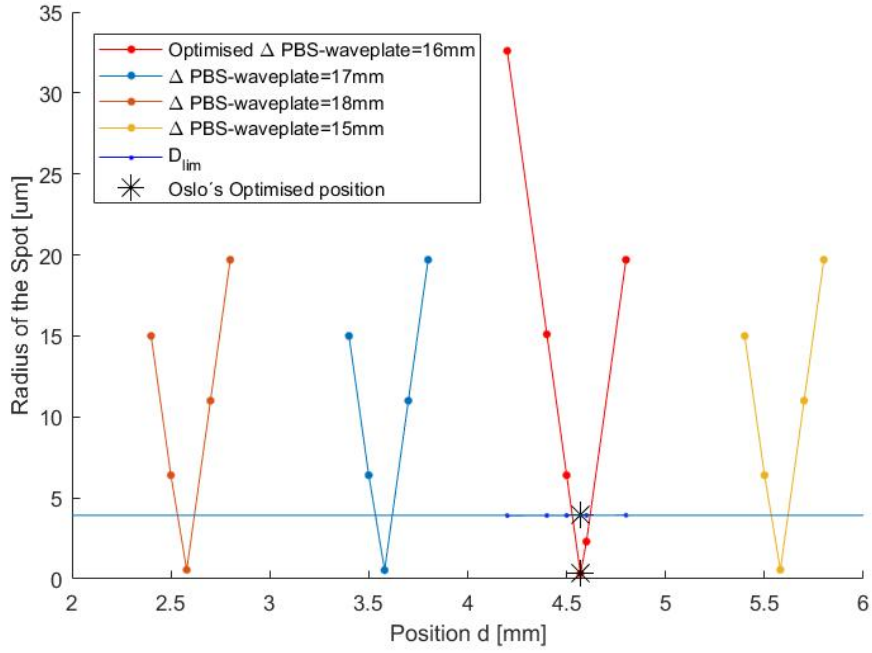


Figure 13: Radius of ray bundle in respect to a distance change between the PBS and objective. The 4 different data plots have different distances between the PBS and the wave plate, which corresponds to surface 10 in 1. It is shown that the system can always be diffraction limited by adjusting the distance between the objective and PBS.

Table 3: Datapoints for figure 13. It can be seen that for every 1 mm the distance between the PBS and waveplate changes the distance between the PBS and objective has to be change 1 mm the other way to obtain the same radius of the ray bundle.

Location ($\Delta 16$)	Radius	Location ($\Delta 17$)	Radius	Location ($\Delta 18$)	Radius	Location ($\Delta 15$)	Radius
4.2	32.6	3.4	15	2.4	15	5.4	15
4.4	15.1	3.5	6.4	2.5	6.4	5.5	6.4
4.5	6.4	3.58	0.54	2.58	0.56	5.58	0.56
4.5699	0.3238	3.7	11	2.7	11	5.7	11
4.6	2.3	3.8	19.7	2.8	19.7	5.8	19.7
4.8	19.7						

Another option with OSLO's spot diagram is to get a figure with several spot diagrams at once, where one can see how the ray bundles are being simulated on the image plane with a focus shift and white a field angle that's not zero, which means that the incoming ray into the optical system starts off at an angle. As before the green points are the imaged rays while the white circle is the airy disk. On figure 14 one can see the different spot diagrams for a maximal focus shift of $10\mu\text{m}$ which is represented as the x-axis. The y-axis displays the difference in angle. Without an angle, the focus is diffraction limited by the airy disk, since all the rays end up inside the circle. This is still true for a shift of $30\mu\text{m}$. However when the rays are tilted by just half a degree comatic aberrations occur and the image is no longer diffraction limited, since some of the rays are outside the circle.

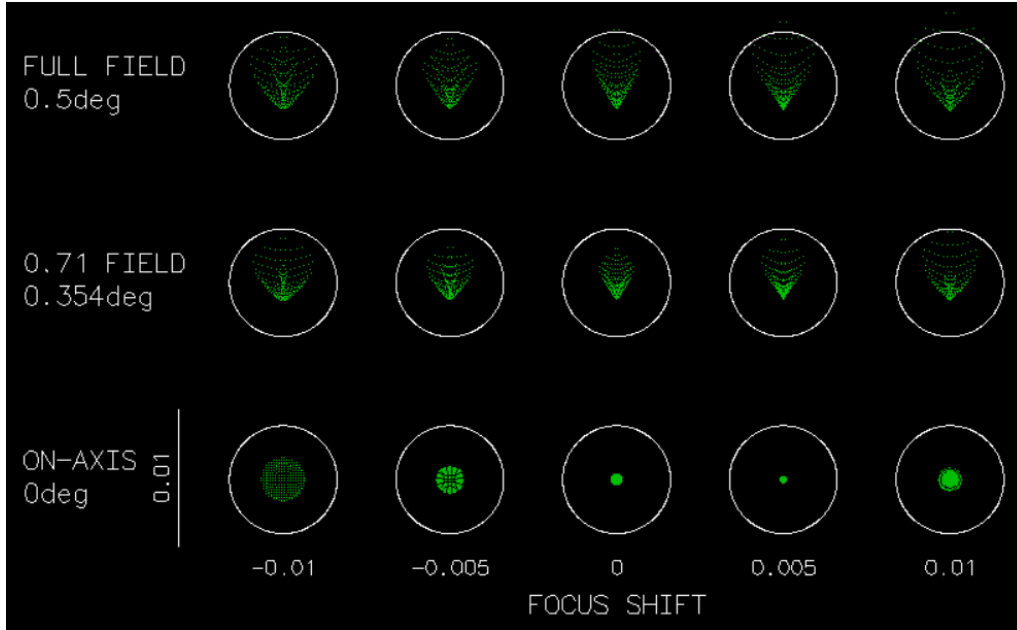


Figure 14: Spot diagram for different shifts in focus and entry degree of the light. On the x axis the focus shifts $5\mu\text{m}$ pr spot. Shown in mm on the figure. On the y-axis is are the values for degree change. When all green point are inside the white circle, which represents the airy disk, the object is diffraction limited.

This is even worse when we look at a tilt of 1 degree, as seen on figure 15

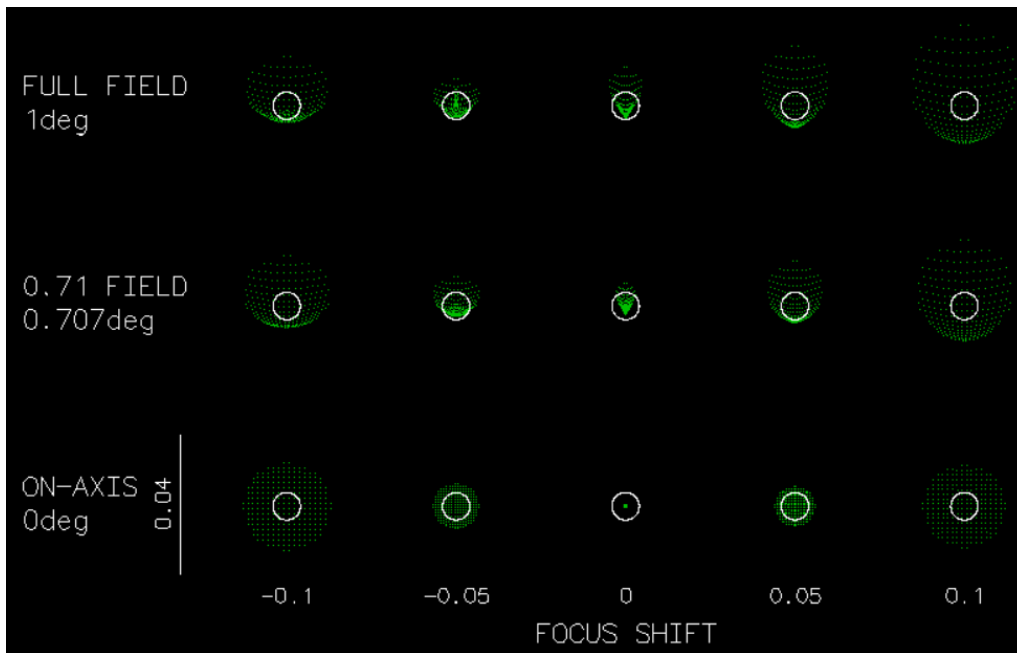


Figure 15: Spot diagram for different shifts in focus and entry degree of the light. A maximal focus shift of 0.1mm and 1 degree angle is shown. The object would be diffraction limited of all the rays end inside the airy disk (white circle)

3.6 Modulation-Transfer-Function

To measure the performance of an imaging system the modulation transfer function (MTF) [Edm92] can be used, which yields a function, which describes the relative contrast at a given resolution. One can use the concept discussed in chapter 3.4 were resolution is defined through black and white resolvable spots. Instead of spots there are used black and white line-pairs like on the USAF

resolution test chart mentioned in chapter 2.1.2. These line-pairs are also called *spatial frequency*, which is a measure of how often sinusoidal structures repeat per given unit of distance. The stripes on the target/object are perfectly black and white with a resulting contrast of 100%. But in real life these stripes aren't imaged as perfect blocks of black or white, but the edges between the change from black an white smear out, since the circular aperture from the lenses used for the imaging result in a circular interference pattern discussed earlier. The closer they these lines come together the more smudged they will be imaged and thereby lose in contrast.

The contrast can be calculated with the following equation:

$$C = \frac{I_{max} - I_{min}}{I_{max} + I_{min}} \quad (17)$$

where I_{max} is the maximum intensity, which equals to a white spot, while I_{min} equals to the minimal intensity, which occurs at a black spot. The lesser the difference the lesser the contrast will be. On Figure 16 the vertical pattern for element 6.2 was taken and through the program ImageJ a plot diagram was created. The possible gray-scale value goes from 0 (black) to 256 (white), which is displayed in the y-axis, while the x-axis shown the location in pixels. The program takes the average of the area to create the plot.

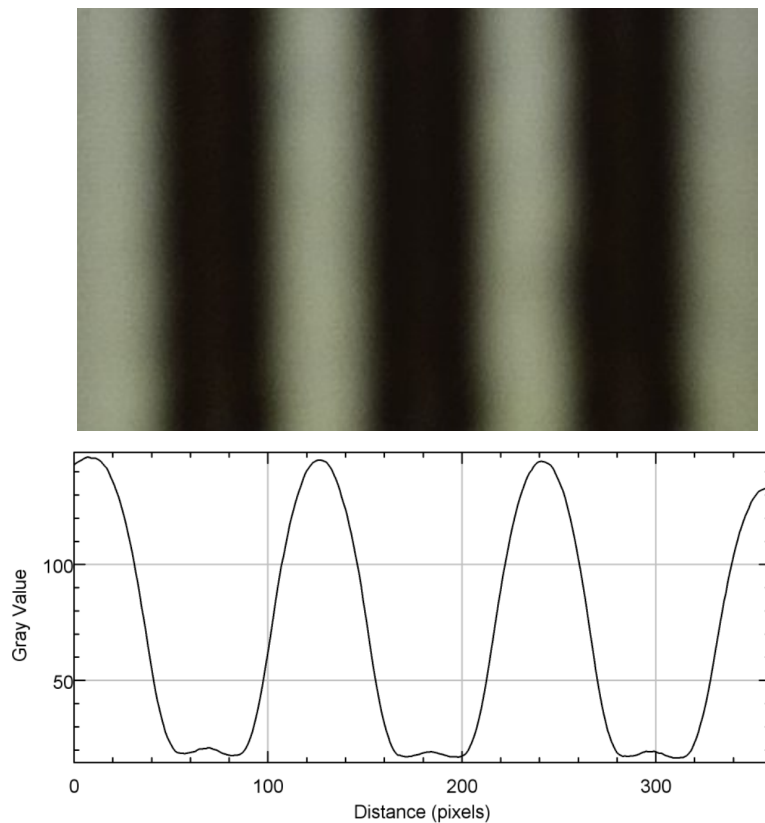


Figure 16: Evaluation of vertical line pattern 6.2. On the top is the line pair 6.2 and on the bottom the corresponding plot diagram. The plot diagram takes the average of the whole areal and evaluates the average grey-value for a given pixel. The program used for the Plot diagram was ImageJ.

Because of a degree of variable uncertainties the calculation of error bars is done through propagation of uncertainty. Our function will be C with the variables being values of I_{min} and I_{max} . The amount of error, uncertainty in the variables true value, is varying depending on Image and resolution. It is suspected that there should be a bigger error without the use of a diffuser. ΔI_{max} and ΔI_{min} are for now chosen to be 10 on the 8-bit grey-scale value. The contrast is seen as a non linear differential function with two independent variables $C(I_{max}, I_{min})$. Through Taylor-expansion the following equation will be used to find the error bars [MR]

$$\begin{aligned}
\Delta C &= \frac{\partial C}{\partial I_{max}} \cdot \Delta I_{max} + \frac{\partial C}{\partial I_{min}} \cdot \Delta I_{min} \\
&= \frac{2I_{min}}{\sqrt{(I_{max} + I_{min})}} \cdot \Delta I_{max} - \frac{2I_{max}}{\sqrt{(I_{max} + I_{min})}} \cdot \Delta I_{min}
\end{aligned} \tag{18}$$

At decreasing distance between the line pairs, at some point one will reach a point where they merge together to a not longer distinguishable gray, where the contrast will go to zero. This is called the cut-off frequency. The MTF in itself will then be a function showing the decline of contrast in correlation to the resolution. This graph depends on the optical system and is showing the competence of the optical system to transfer contrast at a given resolution from an object to an image. On such a graph one can see the modulation on the y-axis and the resolution as the spatial frequency given in line pairs pr millimeter on the x-axis. The MTF calculated by OSLO for the objective can be seen in figure 17.

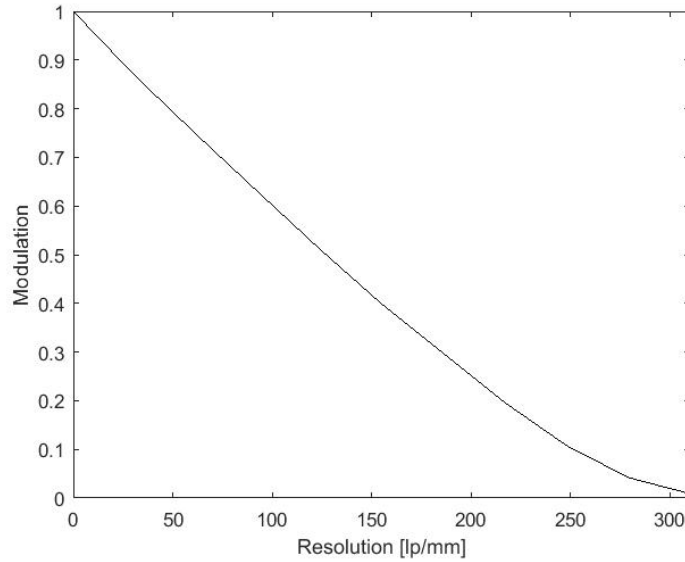


Figure 17: The Modulation transfer function from the target to the end of the objective given by OSLO. The y-axis is the modulation given in contrast going from 0 to 1 for a given resolution defined as line pairs pr mm.

The modulation of the MTF is as shown decreasing for increasing spatial frequency. A contrast of 50% is at around 128 lp/mm, which agrees to the best possible resolution the objective should be able to obtain. On Appendix A it can be read that 128 lp/mm correspond to $3.91 \mu\text{m}$. The cut-off frequency is at 310.45 lp/mm. Considering the groups and elements from the resolution chart, the cut-off frequency corresponds to Element 2 in group 8, which has a lp/mm of 287. But the contrast wouldn't be high enough to be seen as possible achievable resolution through the objective. Noticeable resolution will in this thesis be defined to have at least 50% contrast.

An important fact to consider with MTF's is though, that every component in the optical system has it's own MTF and all of them contribute to the overall MTF of the resulting system. OSLO only takes the surfaces from the resolution target to the end of the objective. Other components which contribute to the overall systems MTF are the focus lens, which is used to refocus the shadow into the camera after the objective, and also the camera sensor. This become important when comparing data to the the MTF obtained through OSLO. It wasn't able to find the MTF from the pi camera.

4 Imaging setup in new mount

This section deals with the analysis of several images taken to characterize the objective and the camera.

4.1 New Set-up

What changed compared to the first set-up is, that the tube consisting of the 4 lenses and the PBS are installed inside the mount. In front of the mount is placed a waveplate, which for this analysis is adjusted so that all the light goes through the PBS into the objective, since its not needed to split the light until the Rydberg experiment. The new set-up can be seen in figure 18 and 19, where the first one is an illustration of the set-up and the second is the set-up in the laboratory. The diffuser was not used in all of the images that were taken with the pi camera. The parts not displayed in the illustration are 2 irises between the 750mm lens and the camera, which don't contribute to the imaged outcome, but help with the alignment, and another component is an empty tube in front of the camera, for reducing the background light. The lights from the ceiling have been extinguish before any picture has been taking. Another thing that changed and provided some kind of complications was the confined space. Since its best to work with straight lines it is se-tup as it is, with a length between the objective and the extra 750mm lens of just 17cm, which preferably should have been 83cm, which corresponds to the focal length of the 750mm lens and the objective added together. Since its the shadow of the target that should be imaged, it shouldn't cause too many problems, as the shadow after the objective is supposed to come out collimated. It would affect it if the objective isn't aligned perfectly and the the shadow doesn't appear parallel. It does affect the amount of light the camera receives, since the light won't be collimated after the objective. The missing length of the table could be avoided by working with mirrors, the issue here is that this would increase the error from possible misalignments. On figure 18 an illustration of the set-up with all the optical components can be seen.

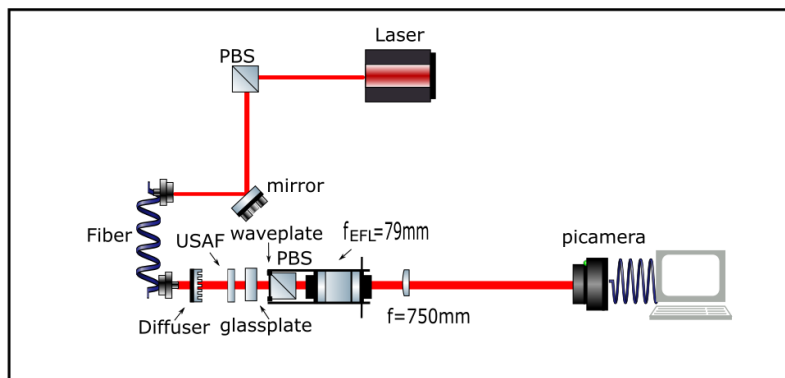


Figure 18: The new set-up for the characterization of the objective. The objective is now in a mount together with the PBS and waveplate.

For some of the future images being described the 750mm lens was replaced with a 500mm lens to get a broader image and to have a bigger distance between the objective and the focusing lens to allow more light from the laser into the camera.

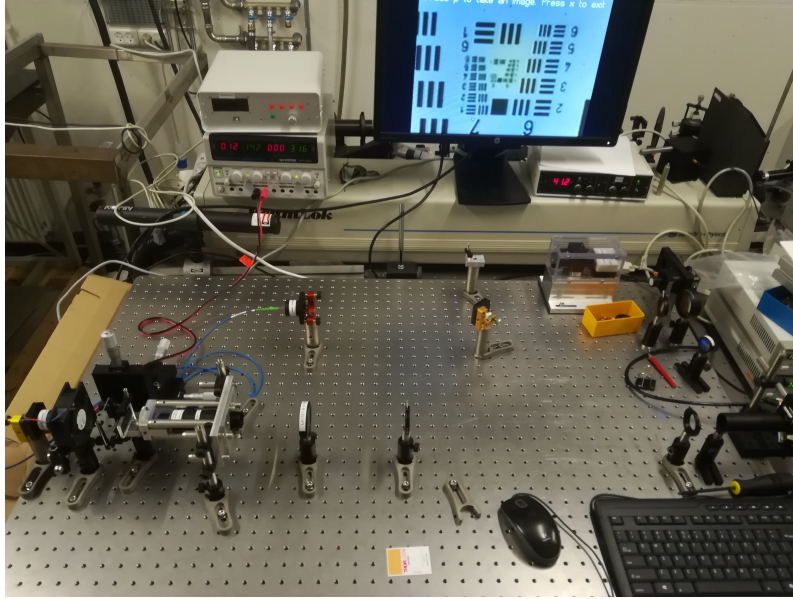


Figure 19: The setup for the characterization as constructed in the laboratory.

4.2 Raspberry Pi-Camera

The Camera used is supposed to have a field of 3280 x 2464 pixels with a pixel size of $1.12\mu\text{m} \times 1.12\mu\text{m}$. To prove the pixel size, the image of the resolution chart can be used. Since it is known what a pixel is supposed to be, this value can be compared with the pixel size measured from the image. Through the look up table from the resolution chart on Appendix A, it is shown, that the size of Element 3 in group 5 is supposed to be $12.4\mu\text{m}$. By taking plot profile of the mentioned line group, one can find out how many pixels the a line in this element corresponds to, which is for the horizontal line is 102px. Now by taking the width of the line in micrometer, dividing it by the amount of pixels it corresponds to and at the end multiplying the result with the magnification of the image, which is 9.4, the pixel size is calculated to $1.131\mu\text{m}$. The same is done for the vertical, which results to a pixel size of $1.131\mu\text{m} \times 1.128\mu\text{m}$, which is similar to the specification. Furthermore a picture with the laser being extinguished has been taken to find the background level, which is found to be around 15-16 in a brightness scale going from 0 to 256.

4.2.1 Location significance

To find out if it makes a difference where on the image a specific pattern is portrayed 4 pictures have been taken, where the pattern is positioned in one of the respective corners and the contrast is measured and compared with each other. The pictures were shot with the 500mm focusing lens and can be seen in figure 20

These images have been taken with the 500mm lens to allow a broader image to move the area of the groups of 6 and 7 to the corners of the picture. It wouldn't have been a big difference to change the whole position of the groups 6 and 7 with the 750mm lens. If one wanted to do the same with the 750mm lens one would have decided on a single pattern to move to each corner and compare the plot diagrams instead of the MTF's. The MTF's of the 4 pictures in figure 20 and for one for the area of interest being in the middle can be seen in figure 21, where the data points when the area is placed in the middle are seen as circles while the data points from the corners are seen as points

It's seen here that the different points for a given line pair are quite spread. The highest spread between data points is for element 6.2, with a spread going from 75% as the lowest data point (corresponding to the bottom right corner image (yellow data points)) to 95% for the highest point (corresponding to the bottom left image (purple data points)).

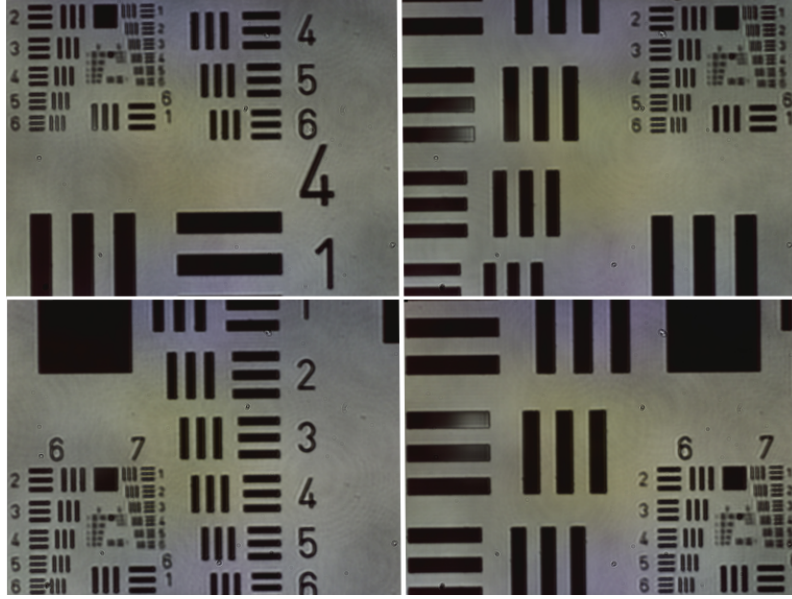


Figure 20: 4 pictures of the resolution chart with the 500mm Lens where the area of interest was moved to each corner to compare the significance of their location.

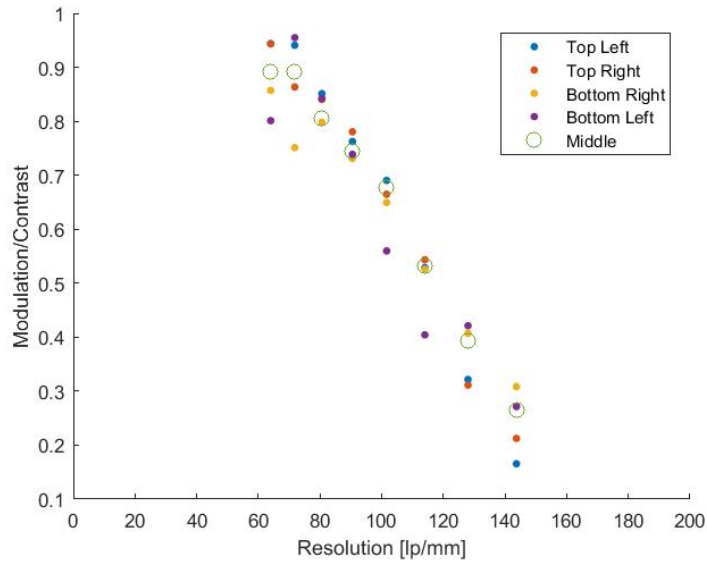


Figure 21: Modulation Transfer Function of the imaging setup with the 500mm lens. The first four (blue,red,orange,purple) are the MTF's for having the area of interest in each of the pattern respectively. The last one called Middle (green circle) is the MTF if the area is placed in the middle of the camera.

4.2.2 Focus shift

This section goes through the effect of small distance changes for between the target and objective, and the camera and the focusing lens. The first figure 22 shows in impact of changing the distance of the target from the optimal position in $20\mu\text{m}$ steps. As a reference for the optimal position one could look at figure 24. It is seen here on figure 22 that already at a change of $20\mu\text{m}$ the element in group 7 start blur up a lot and the smallest elements in group 6 start to show a change. It gets even worse with a larger focus shift. It is mentioned in Chapter Component characteristics and sensitivity, that the resolution is diffraction limited for up to $30\mu\text{m}$. This was though without taking the second lens and the camera into account. But it is also more than likely, that the setup might have some components not perfectly aligned, since it's also seen in Figure 14 that a small

angle has a large effect on the incoming rays. So it's probably the case, that one or more of the components aren't aligned flawlessly.

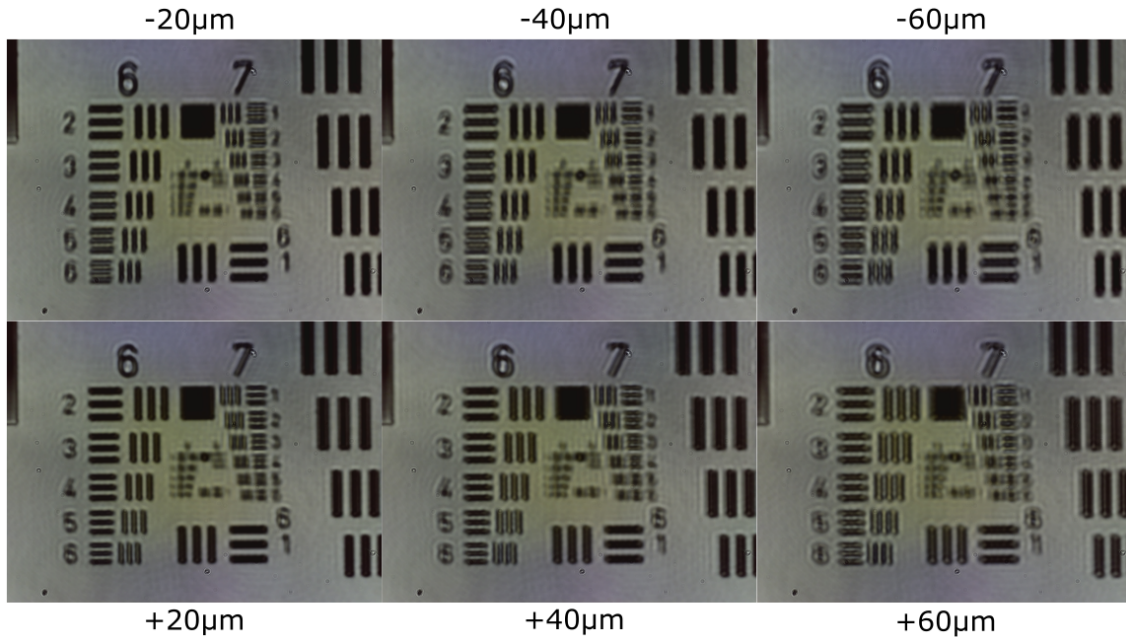


Figure 22: Focus Shift in the target. The images show how to resolution changes per $2\mu\text{m}$ shift in the target toward and away from the objective.

The next figure number 23 shows the focus shift, but from the other side, by moving the camera closer and farther away from the optimal focus point in 0.5mm steps. The effect here isn't as big here, which shows, that the cameras distance not as sensible as the distance between the objective and target, which was expected. The effects of a focus change around 2mm in the camera seem to be close to the same as the ones for $20\mu\text{m}$ in the target

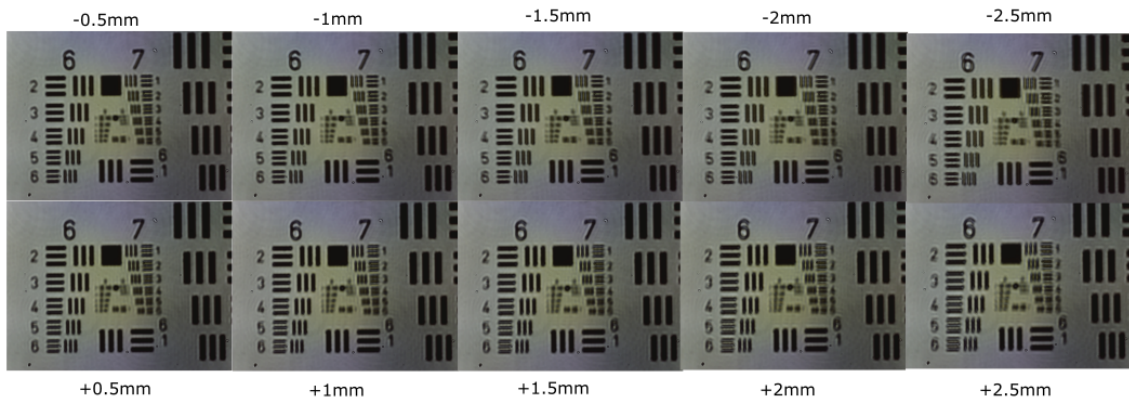


Figure 23: Focus shift in the camera. The images show how to resolution changes per 0.5mm shift in the camera.

4.3 Image analysis

The picture taken through the setup is on figure 24. This picture was taken with the Picamera and the 750mm lens. The light on the picture is not uniform. It is seen to be brighter in the top left corner compared to the mirrored corner. For each of these patterns a contrast is found which form the MTF seen on figure 25.

The black line seen on the figure is the MTF achieved through OSLO's simulations. The blue points are the actual data points obtained from plot diagrams of the various line patterns. The

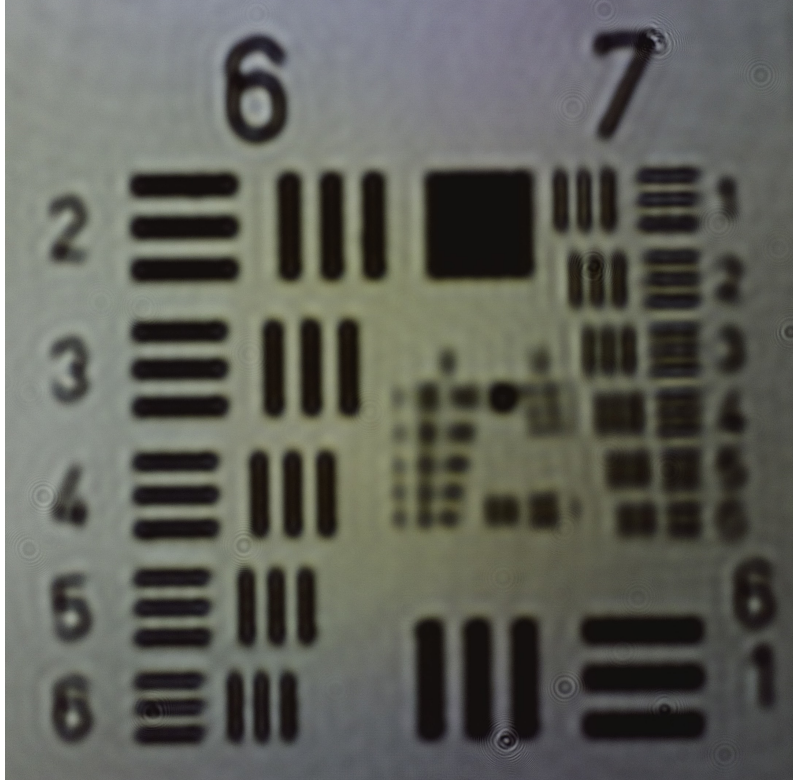


Figure 24: Image of the resolution chart. This is a cropped version of the full image. The Picture was take with the pi camera v2 with a 750mm focusing lens.

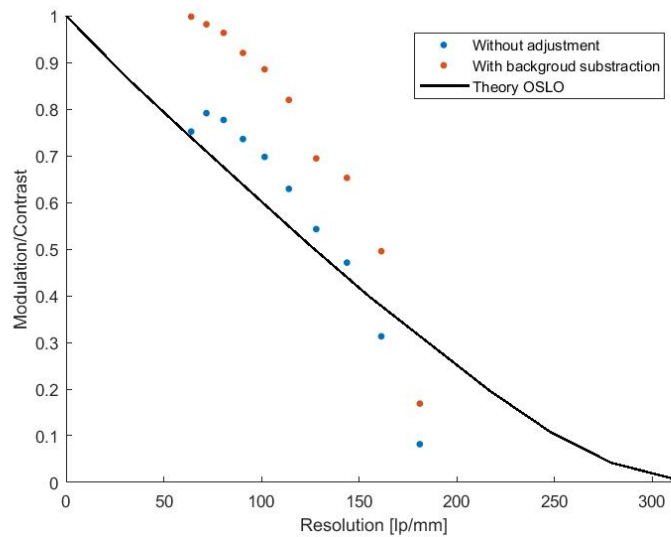


Figure 25: Modulation Transfer function of the imaging setup with the 750mm lens. The blue dots represents the contrast for a given resolution pattern. The red ones display the same data, but with the background subtracted from it. The black line is the MTF given by OSLO for the imaging objective.

red then shows the same data points but with the background subtracted, which is what will be done and shown in further MTF's. Here the original data before the subtraction is pictured to shown the difference it makes to subtract the background. To start of with the blue points, the first data point, which corresponds to element 6.1, doesn't so much follow the other points. The reason for that could be, that the element's location is a distance away from the next point 6.2. Since its darker on the bottom right compared to top left, this could be the reason and was proven

previously in chapter 4.2.1, that this can have such an effect. The reason for the red points being so much above the blues is, that the lowest grey value obtainable from the image is the same as the value being measure at the first line pairs in element 6. Subtracting the background would naturally lead to a contrast of 1. The cause might be because of the cameras response function. A cameras response function [GIN] is a function for the cameras measured intensity in relation to the radiance received. The response function for the Raspberry Pi camera wasn't found, but it could be, that it is poor at distinguish differences in low intensities. It will be investigated later by change the gamma value of the image, which could correct the error, in chapter 4.5. Furthermore there will be used filters for the light to see the different function of MTF for the same image for different amount of light intensities. The data points for both the vertical and horizontal patterns for image 24 can be seen in figure 26. The error bars are calculated with 18.

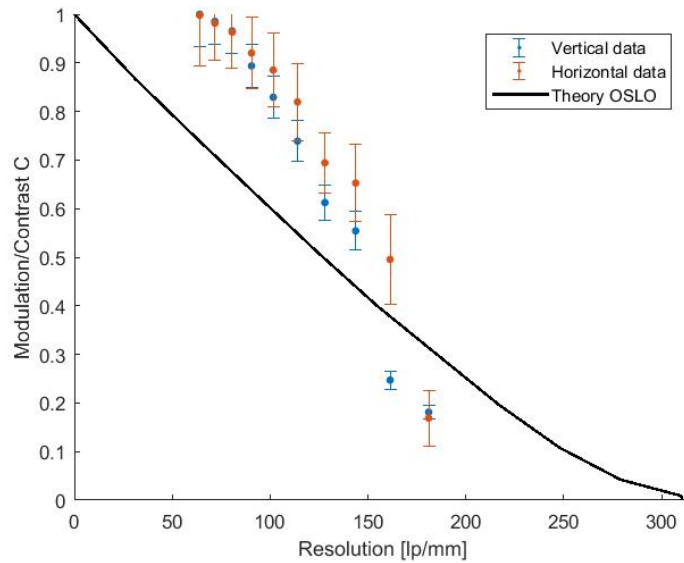


Figure 26: Modulation transfer function of the imaging setup with the 750mm lens from the Vertical (blue) and horizontal (red) line pattern. They display a contrast for a given element on the resolution chart with an error.

Since none of the error bars go through the MTF from the theory, the data have a variation in respect to the theory, either by having the error bars too small, the theory not being correct or the data points aren't right. It can be seen, that the vertical points (blue) in the start are on top of the horizontal (red) but later on deviate from them. That implicates that the system isn't perfectly aligned and that at least the vertical axis has to be aligned better. By a focus shift it would be able to make the contrast of the vertical data better but with the sacrifice in the contrast of the horizontal pattern. In case of the definition of having at least 50% contrast for being counted as the best achievable resolution the best resolution where both vertical and horizontal lines are over the threshold will be element 7.2, which corresponds to a width of $3.48\mu\text{m}$. This is better than expected, even though the not perfectly aligned system. This gives an indication in that the measured contrast might be higher than the actual contrast of the image. In respect to OSLO's sloped seen back in figure 25 the data points are steeper, which also indicate in, that the first few data point lie to high. But if the system were aligned better, the slope wouldn't be as steep as the data shows and there might even have been data for element 7.5.

4.4 Absorptive Neutral Density Filters

In this section the significance for the amount of light going in the camera will be investigated. It is done by placing absorptive Neutral Density (ND) Filters [Opt] in front of the camera. The two filters that are used to limit the amount of light going in the camera are *NE03A* (transmitting 50%) and *NE06A* (transmitting 25%) both from Thorlabs absorptive ND filter kit. The filters are placed more or less directly in front of the camera. Figure 27 shows the result of the use of the 2 filters and one without a filter as a reference. On figure 28 one can see the amount of pixels

having a specific grey value and how it changes for a given filter. The graph indicated as 100% transmission is without a filter. The exposure time for the 3 images was held constant.

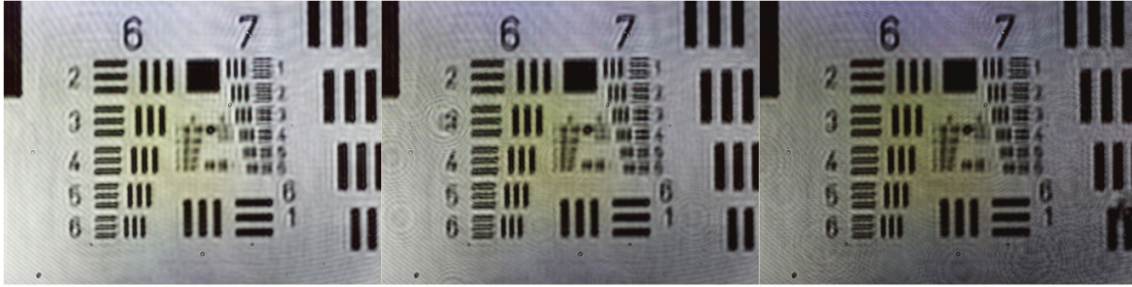


Figure 27: Results of 3 different amount of light transmission through the use of absorptive ND filters. Going from left to right [100%,50%,25%] transmission. 100% transmission indicates, that no filter was used.

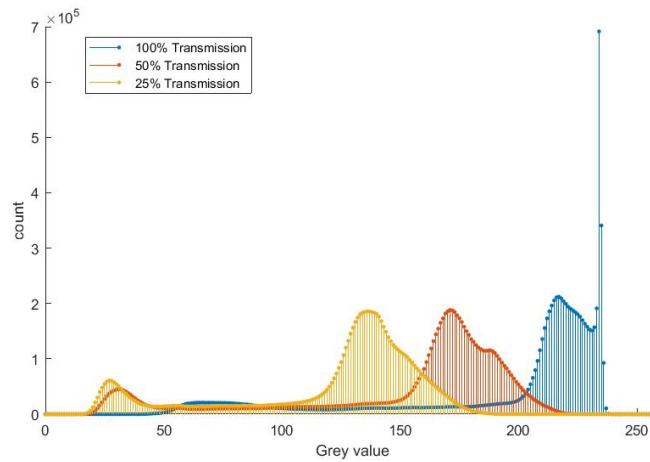


Figure 28: Discrete data plot of the amount of the grey value. There are used ND filters with a 50 % transmission for red and 25% for the yellow plot. The blue data is taken without the use of a filter. The blue one has a high peak close to the limit of the scale which indicates saturation.

The graph shows the 3 different distribution of the gray-scale of the pixels in the images. The image without a filter is shown to have a spike on the right side, which indicates a saturation of light. It also shows a more flat propagation through the darker pixels with the lowest pixels have a grey-scale value of around 36, while the ones with the filter have a elevation at their lowest grey-scale value and their lowest value is around the 15-16 grey-scale mark. The general amount of intensity of the laser has been higher in this test with the filters compared to the laser intensity used to produce the image on figure 24. The saturation has only been noticed after the analysis, but it means that the data for it's MTF can't be used for much. Getting back to the two grey-scale count plots of the two filters, since the light intensity red and yellow was reduced by 50% in respect to each other the grey-scale value should also had been reduced by the same proportion. By taking the two tops at a 171 and 136 the decrease between them is just 21%, which again hints on the camera response function not being linear.

Below on figure 29 the MTF's of the three pictures can be seen. The data points correspond to the horizontal line patterns. The image itself had been sat in focus for the horizontal pattern only, which results in the vertical ones being more out of focus. Neglecting the blue one, the yellow and red ones have no significant difference in the early stages, while later on the red one drops more rapidly. This hints toward, that more light correlate to a lower contrast, but overall getting closer to OSLO's MTF.

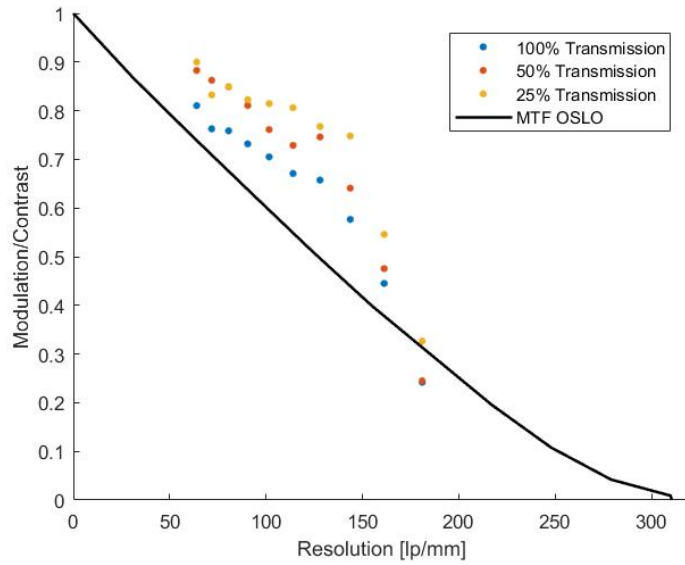


Figure 29: Modulation Transfer Function of the imaging setup with the 750mm lens with the including of filters. It is seen that the MTF is higher for less transmission of the light.

4.5 Gamma correction

As in the previous sections hinted at, could the cameras response function be the reason for a higher than expected contrast. The response function states the correlation between the light that shines on the camera compared to the light one would get out as data from the camera. The relation can be seen as

$$I_{out} = I_{in}^{\gamma} \quad (19)$$

The previous results hint at that the cameras response function isn't linear, but some kind of polynomial. That would mean that $\gamma \neq 1$. Figure 30 shows the correlation between the Intensity going into the camera and the value that would be processed and seen on the image. In comparison to a linear function, it can be assumed that the response function would have a gamma over 1, since the background value is so close to the values of the black stripes, meaning that the camera cant distinguish a difference between low dark colours.

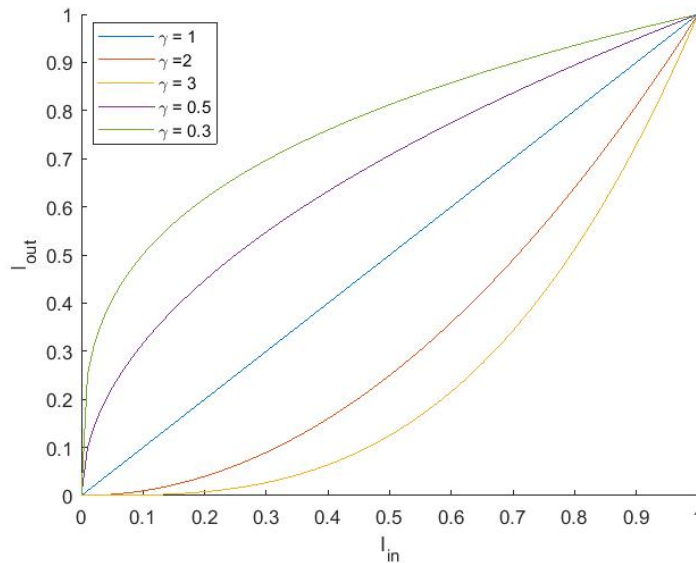


Figure 30: Relation between the in and out going intensity for different gamma values.

A way to correct it, is by changing the gamma value[ic] of the image, which is called gamma correction. Having a gamma correction of gamma below one makes the image brighter and over 1 darker. If the response function would have been known, the correction could have been carried out by the inverse of the gamma from the response function. The camera itself might have had an automatic gamma correction while taking pictures. It is unsure how to access the information about gamma and since the real response function isn't know, two different gamma correction have been tested to see if the data match OSLO's theory better. The values used to test for a correction were $\gamma = 0.75$ and $\gamma = 0.5$ and can be seen on figure 31

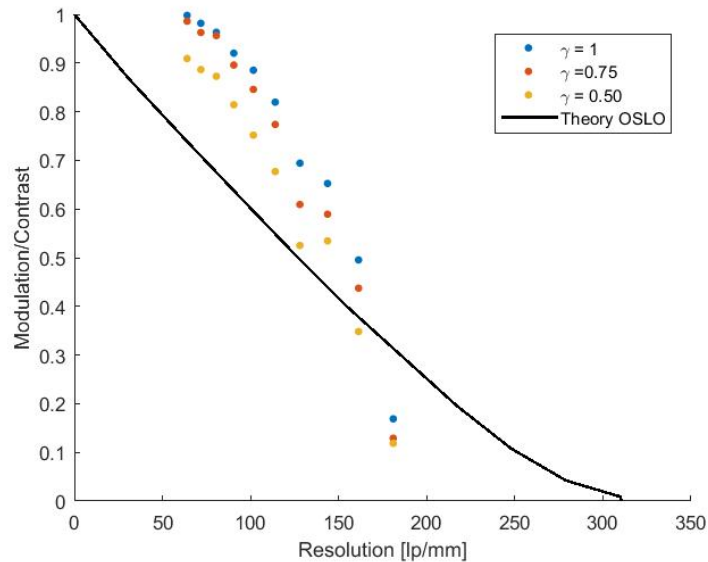


Figure 31: Modulation Transfer Function of the imaging setup with the 750mm with 2 of them being altered through change of the gamma.

But looking at figure 31 one can see the data of the unaltered MTF and two MTF where the gamma value was changed to 0.5 and 0.75. It seems like the altered versions of the same image seem closer to OSLO's MTF. It also shows that all the points lose contrast the more the gamma is altered downwards, making the image brighter. These results suggest that the considerations about the response function are true.

4.6 Diffuser

To remove a lot of interferences a diffuser is added before the light reaches the Resolution chart. On figure 32 a picture of the resolution chart without a diffuser (left) and with it (right) can be seen. The intensity of the laser in both pictures has been the same. It looks like there is more interference on the picture without the diffuser compared to an earlier picture seen in figure 24 with the same set-up. That's because the light intensity of the laser increased after adding the diffuser, since it darkened the picture to let the light pas through a piece of paper. The interference pattern now seen in the new image without a diffuser is also in figure 24, but because the light intensity was lower, it wasn't as visible. The diffuser then destroys most of these by breaking up the Huygen wave-fronts as mentioned in 2.1.2 in section about the diffuser. On figure 33 the plot-diagrams of element 6.5 for both images can be seen. As expected, the interference in the plot is minimal compared to the plot of the pattern without the diffuser. So figure shows, that the spread between the data points is reduced, which has increased the precession.

For the vertical lines of both images in figure 32 a MTF has been made and can be seen in figure 34. The error bars here has been defined with $\Delta=15$ for the image without the diffuser, because of the big changes in the grey-values and $\Delta=5$ for the MTF with the diffuser. The Points of the MTF for the diffuser image is more precise as it seems, where the other MTF is a bit more spread, but does still follow the form of the theoretical function.

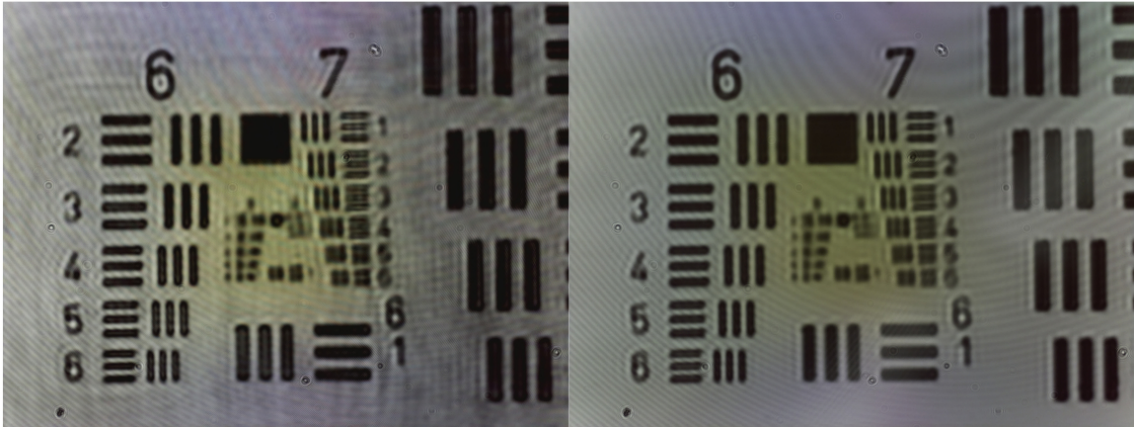


Figure 32: Impact of the diffuser. The image on the right is with a diffuser, the one on the left is without. The laser intensity was the same for both images.

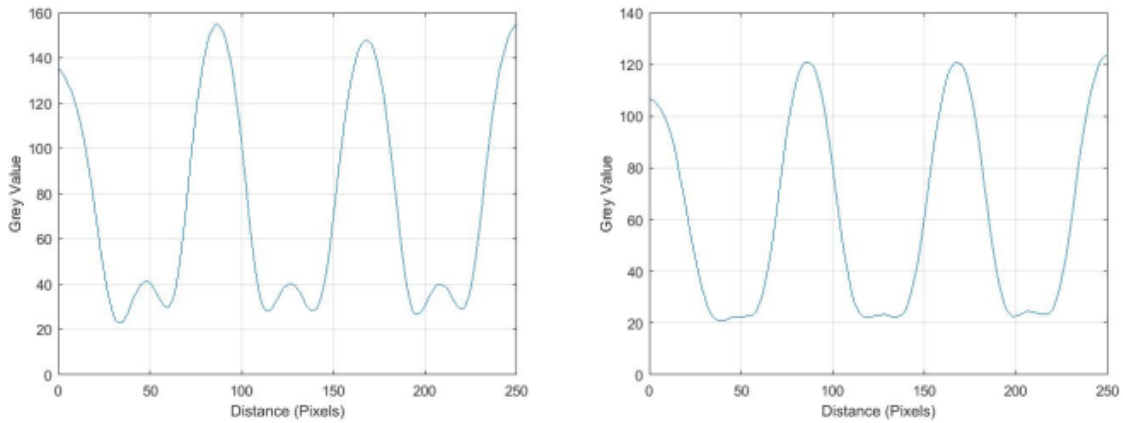


Figure 33: Plot diagram of element 6.5 for the image without diffuser (left) and with diffuser (right). The plots show the average of the grey values for a given pixel given by a areal laid on the pattern of interest.

On figure 35 the MTF's for both vertical and horizontal patterns from the image with the diffuser can be seen together with their corresponding error bars. The first point of the horizontal stripes looks quite far off, this seems because of some interference happening. It can somewhat be seen on figure 32 that the background behind element 6.1 has a bright spot.

Furthermore the points between vertical and horizontal lines are supposed to be close to each other. In the procedure of taking the image, it wasn't aligned perfectly. The focus was shifted a bit to match one of the patterns, which in this case benefited the vertical. This follows, that contrast of the horizontal is lower than it should have been. After the figure above, the best element to have at least 50% contrast would be 7.1, instead of 7.2 which it would have been if one would take the average of the two pattern's MTF in the 7.2, which is over 50%. The use of the diffuser compared to without a diffuser is more accurate toward what the objective will be used for in the Rydberg experiment, which is why this MTF will be taken as the final result. The error bars are also less, compared to figure 26. But to be in agreement with the theoretical MTF, most of the error bars had to be inside if it.

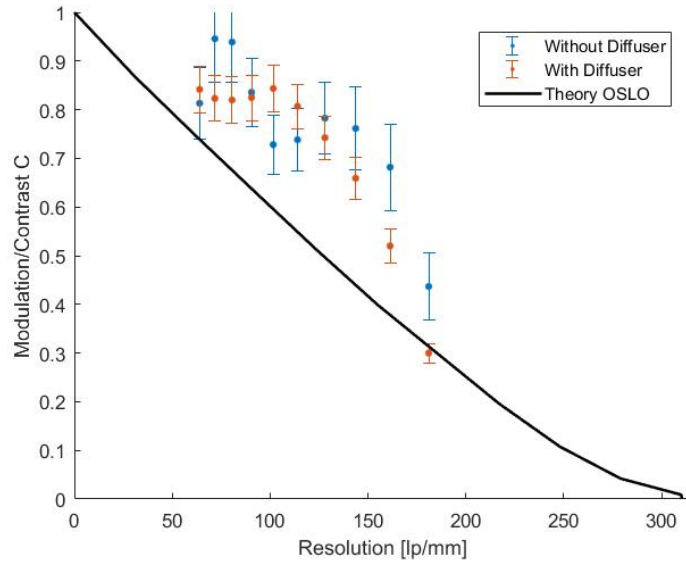


Figure 34: Modulation transfer function of the resolution chart with and without a diffuser for the vertical pattern.

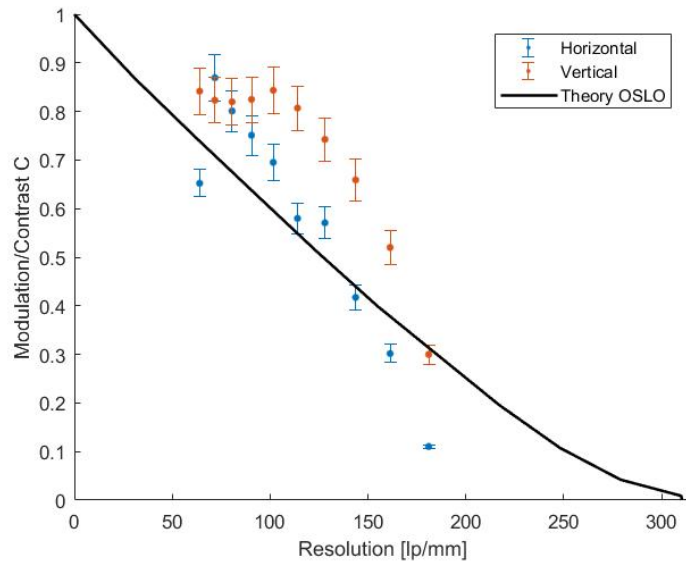


Figure 35: Modulation transfer function of the resolution chart of the vertical and horizontal pattern with a diffuser.

5 Discussion

5.1 Adding of an extra lens

One of the reasons for the results not exactly following the theory could be, because of the illumination on the resolution chart. After a brief talk with F. Christaller, the person who designed the objective, he said that the interference pattern in the background could be erased by having a small lens placed between the diffuser and test plate to focus the light, which after the diffuser is somewhat scattered, back towards the resolution chart. This should give an overall uniform intensity of light in the image, which after his experience should have an impact on the measured contrast of the patterns. This should also lessen the uncertainty shown on figure 20 and 21 where the location of the resolution chart was moved to each of the corners. If there still is a spread, this would then be caused by the sensor of the camera collecting the data different. This might still be the case here, but because of the light difference on the picture it is unsure which effect cause the spread the most.

5.2 Optimized distance between the objective and 750mm lens

Also in the topic of illumination, more light could have been collected by the camera, if the distance between the objective and focussing lens would have been optimal, which is their two focal length added together. This can also be influence on the image itself, if the shadow of the resolution chart after the objective doesn't come out collimated, but with an angle.

5.3 Camera response function

It is unsure what the response function from the camera is, but it is expected to have a slow rise in the beginning, meaning that it's ability to distinguishing various low value grey-scales is quite low. The effect is, that the measured background level is on the same level as some of the grey-scale values of the dark patterns that are being evaluated. Subtracted the background from the close to equal grey value from the pattern would then result in a calculated contrast close to 100%. This was tried to be corrected by applying a gamma correction in after production and seen on figure 31 applying the gamma correction makes the data go towards the from OSLO defined MTF. When Christaller imaged the resolution chart when he design the objective he didn't seem to have the same problems, even though the same camera has been used. This means that the reason could lie somewhere in the options of the camera, which were on automatic mode.

5.4 Diffuser

The Image with the diffuser and its MTF (figure 35) seems to be the best image for defining the best possible resolution obtainable by this set-up. It doesn't posses the same problems with having the contrast in the beginning of the measured MTF of group 6 to be close to 100%. This and the reduced interference make MTF the most reliable one.

6 Conclusion

The best resolution obtained was $3.91\mu\text{m}$, which corresponds to element 7.1 on the 1951 USAF resolution test chart. It was done with the diffuser with the requirements of having at least 50% contrast on both the vertical and horizontal axis. If taking the average of the contrast between the horizontal and vertical axis in account, element 7.2 would be the last applicable pattern, which corresponds to $3.48\mu\text{m}$. The objective has a numerical aperture of 0.1216 with a diffraction limited resolution of $3.91\mu\text{m}$ by the Abbe diffraction limit, which is in a agreement with having element 7.1 as the last element. Comparing OSLO's MTF with the MTF from the data, shows that the data has a steeper downward slope resulting in a faster cut-off, meaning that it has no contrast. This is likely due to imperfect alignments of some of the components. The Results from the MTF and several analysis's throughout the thesis show that the contrast measured from the data in some of the first patterns of group 6 is higher than what it should have been. It is expected to be due to the cameras response function.

7 Acknowledgment

I would firstly like to thank my 2 supervisors Sebastian Hofferberth from the institution of pharmacy, chemistry, and physics, and René L. Eriksen from the Faculty of Engineering on Southern Denmark University. Their door were always open whenever I ran into trouble and they steered me in the right direction for writing this thesis.

I would also like to to thank the members the NQO research group in SDU, S. W. Ball, C. Braun, P. Lunt, N. Stiesdal, and C. Tresp to whom I'm grateful for all the good input they gave me and for also sharing some pleasant time together.

Finally, i would like to thank my family and friends for their unfailing support and encouragement through my years of study.
Thank you.

Tom M. B. Asmussen

References

- [Alt02] Wolfgang Alt. An objective lens for efficient fluorescence detection of single atoms. *Optik - International Journal for Light and Electron Optics*, 113(3):142–144, jan 2002.
- [Che] Alan Cheville. Modulation Transfer Function. <https://www.youtube.com/watch?v=1VgqsMqBpKc>. (20/05/18).
- [Chr17] Florian Christaller. Construction and setup of a 3rd generation Rydberg Quantum Optics experiment. 2017.
- [Cos] Cosmos indirekt 14-05-18. Hauptebene (Optik).
- [Edm92] Edmund Optics. Introduction to Modulation Transfer Function, 1992.
- [GIN] Michael D. Member Grossberg, IEEE, and Shree K. Nayar. Determining the Camera Response from Images: What Is Knowable?
- [ic] Cambridge in colour. UNDERSTANDING GAMMA CORRECTION (28/05/18).
- [Lam12] Lambda Research Corperation. OSLO Optics Reference. (June):427, 2012.
- [MR] Douglas C Montgomery and George C Runger. *Applied Statistics and Probability for Engineers Third Edition*.
- [Opt] Edmund Optics. Absorptive Neutral Density (ND) Filters.
- [PIS⁺17] J D Pritchard, J A Isaacs, M Saffman, J D Pritchard, J A Isaacs, and M Saffman. Long working distance objective lenses for single atom trapping and imaging Long working distance objective lenses for single atom trapping and imaging. 073107(2016), 2017.
- [PPP] Frank L Pedrotti, Leno M Pedrotti, and Leno S Pedrotti. Introduction to Optics 3/E.
- [SZD⁺17] Tim Stangner, Hanqing Zhang, Tobias Dahlberg, Krister Wiklund, and Magnus Andersson. A step-by-step guide to reduce spatial coherence of laser light using a rotating ground glass diffuser. pages 1–8, 2017.

A 1951 USAF resolution test chart look up table

Width of 1 line in micrometers in USAF Resolving Power Test Target 1951												
Element	Group Number											
	-2	-1	0	1	2	3	4	5	6	7	8	9
1	2000.00	1000.00	500.00	250.00	125.00	62.50	31.25	15.63	7.81	3.91	1.95	0.98
2	1781.80	890.90	445.45	222.72	111.36	55.68	27.84	13.92	6.96	3.48	1.74	0.87
3	1587.40	793.70	396.85	198.43	99.21	49.61	24.80	12.40	6.20	3.10	1.55	0.78
4	1414.21	707.11	353.55	176.78	88.39	44.19	22.10	11.05	5.52	2.76	1.38	0.69
5	1259.92	629.96	314.98	157.49	78.75	39.37	19.69	9.84	4.92	2.46	1.23	0.62
6	1122.46	561.23	280.62	140.31	70.15	35.08	17.54	8.77	4.38	2.19	1.10	0.55

Number of Line Pairs / mm in USAF Resolving Power Test Target 1951												
Element	Group Number											
	-2	-1	0	1	2	3	4	5	6	7	8	9
1	0.250	0.500	1.00	2.00	4.00	8.00	16.00	32.0	64.0	128.0	256.0	512.0
2	0.281	0.561	1.12	2.24	4.49	8.98	17.96	35.9	71.8	143.7	287.4	574.7
3	0.315	0.630	1.26	2.52	5.04	10.08	20.16	40.3	80.6	161.3	322.5	645.1
4	0.354	0.707	1.41	2.83	5.66	11.31	22.63	45.3	90.5	181.0	362.0	724.1
5	0.397	0.794	1.59	3.17	6.35	12.70	25.40	50.8	101.6	203.2	406.4	812.7
6	0.445	0.891	1.78	3.56	7.13	14.25	28.51	57.0	114.0	228.1	456.1	912.3

Figure 36: Lookup table for resolution with respect to the correlated element in a given group. The most upper one shows the width of a single line and the bottom one shows the number of line pairs per mm.

B Table of ray-transfer matrices

SUMMARY OF SOME SIMPLE RAY-TRANSFER MATRICES	
<p>Translation matrix:</p> $M = \begin{bmatrix} 1 & L \\ 0 & 1 \end{bmatrix} = \mathfrak{T}$	
<p>Refraction matrix, spherical interface:</p> $M = \begin{bmatrix} 1 & 0 \\ \frac{n-n'}{Rn'} & \frac{n}{n'} \end{bmatrix} = \mathfrak{R}$	<p>(+R) : convex (-R) : concave</p>
<p>Refraction matrix, plane interface:</p> $M = \begin{bmatrix} 1 & 0 \\ 0 & \frac{n}{n'} \end{bmatrix}$	
<p>Thin-lens matrix:</p> $M = \begin{bmatrix} 1 & 0 \\ -\frac{1}{f} & 1 \end{bmatrix}$ $\frac{1}{f} = \frac{n' - n}{n} \left(\frac{1}{R_1} - \frac{1}{R_2} \right)$	<p>(+f) : convex (-f) : concave</p>
<p>Spherical mirror matrix:</p> $M = \begin{bmatrix} 1 & 0 \\ \frac{2}{R} & 1 \end{bmatrix}$	<p>(+R) : convex (-R) : concave</p>

Figure 37: Summary of some simple ray-transfer matrices. Taken from Chapter 18 of [PPP]

C Significance of vanishing ray-transfer matrix elements

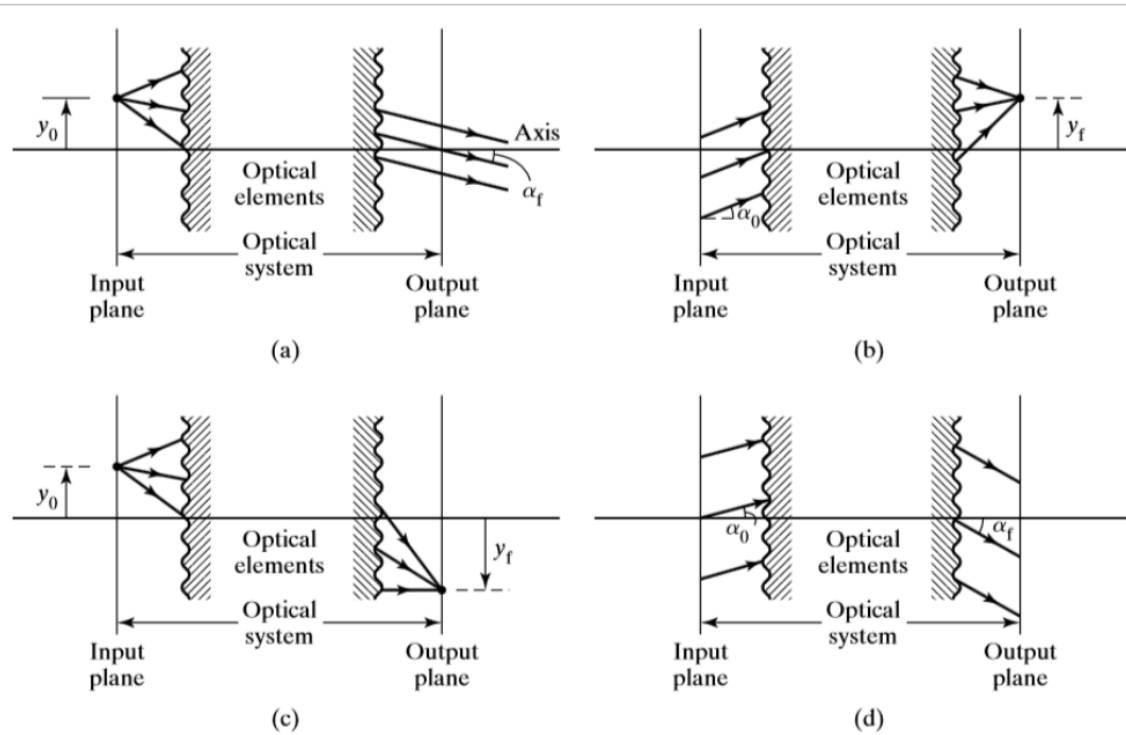


Figure 38: 4 illustrations showing the significance of the disappearing of specific matrix elements. $D=0$ in (a), $A=a$ in (b), $B=0$ in (c), and $C=0$ in (d). Taken from Chapter 18 of [PPP]

D Cardinal points table

CARDINAL POINT LOCATIONS IN TERMS OF SYSTEM MATRIX ELEMENTS		
$p = \frac{D}{C}$	F_1	} Located relative to input (1) and output (2) reference planes
$q = -\frac{A}{C}$	F_2	
$r = \frac{D - n_0/n_t}{C}$	H_1	
$s = \frac{1 - A}{C}$	H_2	
$v = \frac{D - 1}{C}$	N_1	
$w = \frac{n_0/n_t - A}{C}$	N_2	
$f_1 = p - r = \frac{n_o/n_t}{C}$	F_1	} Located relative to principal planes
$f_2 = q - s = -\frac{1}{C}$	F_2	

Figure 39: A table about how to use the matrix elements to find the cardinal points. Taken from Chapter 18 of [PPP]

E Image of resolution chart obtained by F. Christaller

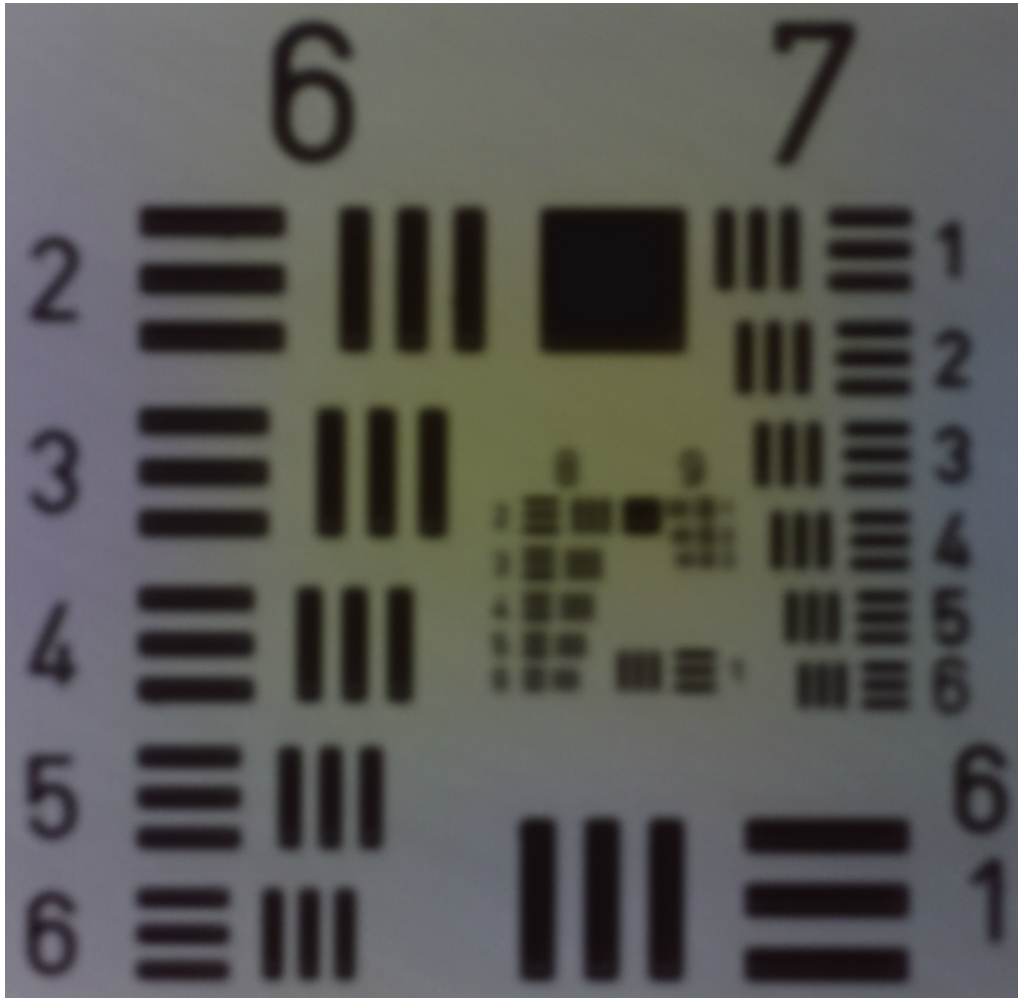


Figure 40: Image of the resolution chart obtained by F. Christaller [Chr17]

F Acronyms

PBS	Polarizing beamsplitter
BS	Beamsplitter
OSLO	Optical software for layout and optimization
RO	Real object
RI	Real Image
EFL	Effective focal length
FF	Front focus
BF	Back focus
NA	Numerical aperture
Px	Pixel
MTF	Modulation transfer function
ND	Neutral density

G List of symbols

M	Magnification
s'	Distance from lens to image
s	Distance from objective to lens
F	Focal length
f_0	Focal length of the objective
f_e	Focal length of the eyepiece
f_{Fcs}	Focal length of the focussing lens
f_{EFL}	Effective focal length of the objective
y_f	Height of the outgoing ray
α_f	Angle of the outgoing ray
\mathbf{M}	Ray-transfer matrix
y_0	Height of the incoming ray
α_0	Angle of the incoming ray
A,B,C, and D	Matrix elements
H	Principal point
N	Nodal point
$\mathbf{M}_{objective}$	Ray-transfer matrix calculated from the start of target to the end of the objective
θ_{min}	Angle needed for the first minimum on the airy disk
λ	Wave length of the laser light
D	Diameter of the lens' aperture
x_{min}	Minimum distance between two objects to be distinguishable
n	Refractive index of the medium the lens is set in (n=1 in air)
R	Resolution
G_{rms}	Geometrical rms value from the radius of the ray bundle in the spot diagram
D_{lim}	Theoretical limit of angular resolution. Everything below is diffraction limited
C	Contrast
I_{max}	Maximal intensity, located between the black stripes
I_{min}	Minimal intensity, located in the black stripes.
ΔC	Interval of uncertainty in the contrast.
γ	Value of the gamma correction